Petrogenic Significance of Ultrabasic Inclusions in Basaltic Rocks from Southwest Japan

Yamaguchi, Masaru
Faculty of Science, Kyushu University

https://doi.org/10.5109/1543617

出版情報：九州大學理學部紀要 : Series D, Geology. 15 (1), pp.163-220, 1964-06-25. Faculty of Science, Kyushu University
バージョン：
権利関係：

Mem. Fac. Sci., Kyushu Univ., Ser. D, Geology, Vol. XV, No. 1,
pp. 163-219, 19 text-figs., 12 tables, plates 22-26, May 31, 1964

Petrogenic Significance of Ultrabasic Inclusions in Basaltic Rocks from Southwest Japan

By

Masaru YAMAGUCHI

Abstract

About three hundred rock specimens of peridotitic and gabbroic rocks enclosed in basalts and limburgites of Chugoku and north Kyushu, Southwest Japan, have been examined petrographically. The constituent minerals separated from these inclusions, clinopyroxene in particular, were studied in detail by chemical and X-ray methods and packing indices of the clinopyroxenes were calculated to compare with those from other sources.

The inclusions examined differ in their rock types among different places, different host rocks, and no longer stable in their host rocks showing disintegration and reaction. They are generally characteristic of strongly deformed structure due to translation, or of wavy extinction, in olivine and pyroxenes. Of these characteristics, complicated exsolution patterns in clinopyroxenes and orthopyroxenes are of great petrogenic significance.

Clinopyroxenes in these inclusions are highly remarkable for a large proportion of Al replacing Si in the structure and for their smaller cell volume than those in other igneous rocks. The highest packing index of clinopyroxene from ultrabasic inclusion is noted. These evidences are well represented in terms of packing index to the number of 2−Si atoms, which indicate the possibility that the packing index may be used as a key of geological barometer.

The noticeable similarity in mineralogy and petrographic character between ultrabasic inclusions and ultrabasic intrusive rocks has led some writers to adhere to the current view that the upper parts of the earth's mantle are made up of peridotites which are found in the accessible crust. However, packing index of clinopyroxene and other crystal-chemical features indicate that most ultrabasic inclusions are derived from greater depths, comparatively deeper than the source of peridotite intrusives, where a layered structure is developed, different layers being composed of different varieties of ultrabasic rocks which are strongly deformed. The differences in layer of the mantle where partial remelting could occur are probably responsible for variation in composition of basaltic rocks.

Contents

Submitted 26 September, 1961; revised manuscript received 18 November, 1963

List of Tables

List of Illustrations

Introduction

The mode of origin and upsurge of basaltic magmas are questions which still afford matter for controversy. Of many opinions hitherto put forth, some have been abandoned, others remains, though modified in part by modern precise studies, appearing in current literature in various languages. Production of basaltic liquid by partial remelting of the 'peridotite layer' first discussed by BOWEN (1928) has been the prevailing conception. Thus, ROSS and others (1954) have recognized the similarity of chemical and mineral compositions between the olivine-rich inclusions in basaltic rocks and intrusive dunites of world-wide distribution. POWERS (1955) put strong emphasis on the conception on the seismological and volcanological evidences in the Hawaiian Volcanoes, and KUNO (1953, 1959a, 1960) exaggerated the idea to the origin of Cenozoic petrographic provinces of Japan and surrounding areas. However, the petrological significance of the "olivine nodules" in basaltic rocks is still an open question as to whether they have been derived directly from a primary peridotite zone. TOMITA (1958) indicated the possibility of the presence of gabbroic rock at depth of the Hawaiian volcanoes. Again, the laboratory work of TILTON and others (1956) on the contents of uranium, thorium, lead and isotopic composition of the lead in several

nodules as well as in one host basalt, does not prove, as LOVERING (1959) stressed, that the nodules are fragments of the earth's mantle. Recently, WILSHIRE and BINNS (1961) have concluded that the basic and ultrabasic xenoliths represent unmelted fragments of the mantle, while O'HARA and MERCY (1963) have revived the conception that the nodules are of igneous origin.

On the other hand, there are some other assumptions concerning the mode of origin of magmas as follows: Complete melting of a solid eclogite layer which is high-density equivalent of basalt (FERMOR, 1914); periodic melting of a solid basaltic layer under the influence of radioactive heat (JOLY, 1925); complete melting of respective granitic, basaltic and peridotitic layer (HOLMES, 1933); selective fusion of various silicate rocks (ESKOLA, 1933), and finally in the most modern state, partial remelting of a more primitive rocks (e.g. garnet peridotite) (YODER and TILLEY, 1962).

The Mohorovičič discontinuity has long been considered as a boundary between two layers of different compositions basalt and peridotite (WAGER, 1958), not a few investigators now believe that the discontinuity is due to a phase change, basalt-eclogite transformation (BUDDINGTON, 1943; LOVERING, 1958; YODER and TILLEY, 1962).

Since the mantle is beyond our direct observation, the practical problem to petrologists would be intensive and extensive studies of peridotitic and gabbroic inclusions in basaltic rocks which may afford the direct evidence of the birth place and the process of formation of basalt magma.

For the solution of this problem, comparison of these inclusions with peridotitic intrusive rocks would be at least an important step. Further, the fact that most ultrabasic inclusions have been found in the olivine basaltic rocks of alkaline affinity, may be interpreted in view of the fact that these inclusions are nearly absent in the tholeiitic olivine basaltic rocks. For this reason, intrusive ultramafic rocks from several localities in Japan, and other basaltic rocks without xenolithic ultrabasic rocks have also been examined in comparison with the ultrabasic inclusion.

I have collected about three hundred specimens of peridotitic and gabbroic inclusions in basalts and limburgites distributed in Chugoku and North Kyushu, southwestern Japan. These materials have been examined by petrographic, chemical and X-ray methods, and the results are incorporated and discussed in this paper.

Acknowledgements

I wish to express my best thanks to Professor Tôru TOMITA of our Department, for his discussion and criticisms throughout the study and preparation of this paper, for his kind help in collecting the inclusions from Takashima Islet in the Bay of Karatsu, and for his kindness in reading the manuscript.

My hearty thanks are due to Dr. Atsuo HARUMOTO, formerly Professor of Kyoto University, for his kind information on the locality of nodule-bearing

basaltic rocks from Okayama Prefecture, to Dr. Takashi KATSURA of the Tokyo Institute of Technology, for his kind help with chemical analyses, to Drs. Tsunehiko ÔSHIMA and Hirosato YAMAMOTO of Saga University and Fukuoka Gakugei University respectively, for their cooperation during the study of ultramafic intrusive rocks.

I am also grateful to Professor Toyofumi YOSHIMURA of our Department, who gave me peridotite samples from Sanushibe, Horoman, Hokkaido, to Drs. Yoshifumi KARAKIDA, Hitoshi MOMOI of our Department and Mr. Kiyoshi ISHIBASHI of Ehimé University, who helped me in collecting the nodules in the basalt from Karatsu, to Dr. Yoshimasu KURODA of Tokyo Kyoiku Daigaku (Tokyo University of Education) and Dr. Michitoshi MIYAHISA of Ehimé University, who supplied me samples of olivine gabbro inclusion in basalt from Mikura-zima Islet, south of Tokyo, and of peridotite from Obira Mine, respectively.

Further I wish to express my thanks to Professors Hisamichi MATSUSHITA, Tatsuro MATSUMOTO, Ryuzo TORIYAMA and Dr. Sadakatsu TANEDA of our Department, for their valuable advice and encouragement during the study. Several pyroxene samples preserved in our laboratory collected by the late Professor Kenichi SUGI and the late Professor Sokichi KOO were of great value in the present study.

This study was partly financed by the Grant in Aid for Scientific Researches from the Ministry of Education, Japan.

I. Geology and Petrography of Ultrabasic Inclusions in Basalts and Limburgites from Southwest Japan

1. Distribution of Ultrabasic Inclusion

The peridotitic and gabbroic inclusions in basaltic rocks from Japan, although occasionally found in the literature (AOYAMA, 1942; HARUMOTO, 1952; ROSS and others, 1954) have never been studied systematically. The distribution of the inclusions in basaltic rocks and limburgitic rocks from Japan, which were mostly obtained by myself in the field survey, is shown in Fig. 1. The rock types and the frequency of these inclusions are given in Table 1 and the chemical compositions of host rocks in Table 2. Brief notes on the occurrence of these inclusions in each locality are given below.

2. Dôgo, Oki Islands in the Japan Sea

Detailed studies on the geology and petrology of the Tertiary and recent volcanic rocks from Dôgo have been accomplished by TOMITA (1927-1932, 1935, 1936).

The second trachy-basalt flow (Pleistocene, TOMITA 1936), about 20 meters thick, encloses fairly abundant inclusions at the quarry of Shimo-ganya, northern sea-shore of Dôgo Island. The basalt has attracted our special attention since it contains pseudo-hypersthene as phenocrysts and potash-andesine in the groundmass which have already been described in detail by TOMITA (1935, 1936).

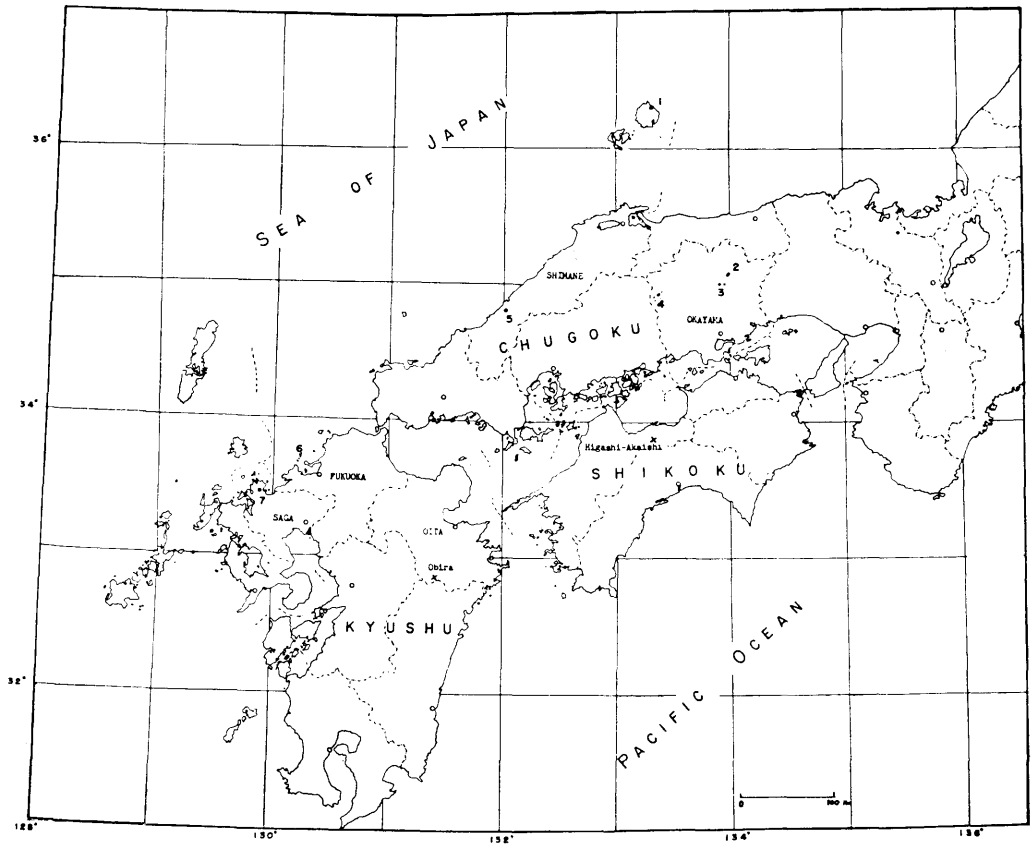

Fig. 1. Index map showing the distribution of ultrabasic and basic inclusions in basaltic and limburgitic rocks from Southwest Japan
1. Shimo-ganya, Dogô; 2. Oyama and Meyama; 3. Sukumozuka and Kajiko-yama; 4. Nochi; 5. Ôguso yama; 6. Kurose; 7. Takashima Islet and other places in the Karatsu area

The basalt, light grey or greyish black in colour, is porphyritic with sporadic large phenocryst of labradorite (20 mm in maximum length) and ortho-pyroxene (pseudohypersthene) and normal phenocryst of olivine and augite.

The inclusions collected from the new cutting, more than one hundred in number and ranging from several milimetres to fifteen centimetres in size, are divided into several rock types as is shown in Table 1 (Plates 22-23).

Optical properties of constituent minerals of each rock type are presented in Table 3; brief notes on the constituent minerals of each rock type are given in the following.

Olivine in peridotite inclusions (Wehrlite and Harzburgite) is unhedral clear crystals with no zoning, often showing distinct translation lamellae parallel to (100). Sometimes, it is included in augite or bronzite.

Olivine in olivine gabbro or augite olivine gabbro is usually small rounded grains, often included poikilitically in the large plagioclase crystals. Translation

Table 1. Rock types and frequency of basic and ultrabasic inclusions in basalts and limburgites from Southwest Japan

Locality (Host rock)	Rock type		Constituent mineral	Approximate frequency in per cent.
Shimo-ganya, Dôgo, Oki Islands (Olivine-basalt)	Wehrlite (Diallage peridotite)		Olivine, augite, picotite, with or without small amounts of plagioclase	10
	Harzburgite (Bronzite peridotite)		Olivine, bronzite and picotite	5
	Websterite		Augite, bronzite and picotite	10
	Bronzitite		Bronzite	5
	Olivine gabbro		Olivine, plagioclase	30
	Augite-olivine gabbro		Olivine, augite, plagioclase	40
Oyama and Meyama (Limburgitic basalt)	Wehrlite		Olivine, chrome-diopside and picotite	100
Sukumozuka and Kajikoyama (Limburgite)	Dunite		Olivine and picotite	98
	Diallagite		Diopsidic augite	2
Nochi and its environs (Picrite basalt)	Harzburgite		Olivine and bronzite	20
	Websterite		Diopsidic augite and bronzite	80
Ôgusoyama (Limburgite)	Dunite		Olivine and picotite	15
	Wehrlite		Olivine, chrome-diopside and picotite	80
	Diallagite		Diopsidic augite	5
Kurose (Olivine basalt)	Wehrlite		Olivine, augite and picotite	50
	Harzburgite		Olivine, bronzite and picotite	50
Takashima and its environs (Olivine basalt)	Dunite		Olivine and picotite	40
	Peridotite	A	Olivine, chrome-diopside and picotite	22
		B	Olivine, augite, bronzite and picotite	10
	Diallagite & Websterite		Diopsidic augite and picotite with or without small amounts of olivine or bronzite	14
	Gabbro	A	Augite, plagioclase, hercynite and olivine	4
		B	Augite, bronzite, plagioclase and hercynite	10

Table 2. Chemical compositions of basaltic and limburgitic rocks enclosing ultrabasic rocks, Southwest Japan

Sample No.	1	2	3	4
SiO_2	49.03	43.26	43.80	42.93
Al_2O_3	14.43	13.40	12.54	10.71
Fe_2O_3	1.29	3.06	4.68	6.03
FeO	9.40	8.36	7.35	6.14
MgO	11.93	11.98	10.85	11.48
CaO	7.28	11.76	12.34	11.21
Na_2O	3.14	3.44	2.58	2.42
K_2O	1.24	1.03	1.26	1.98
H_2O (+)	0.73	1.11	1.21	2.78
H_2O (−)		0.71	0.48	
TiO_2	1.71	1.75	2.70	2.48
P_2O_5	0.44	0.55	0.45	1.38
MnO	tr.	0.21	0.18	1.23
Total	100.62	100.62	100.42	100.77
Analyst	K. YOKOYAMA	A. HARUMOTO	N. KOKUBU & M. YAMAGUCHI	K. YOKOYAMA
Reference	TOMITA (1935)	HARUMOTO (1951)	New analysis	TOMITA (1935)

1. Pseudohypersthene-bearing olivine basalt, Shimo-ganya, Naka-mura, northern sea shore of Dôgo Island in the Japan Sea (KOZU, 1913; TOMITA, 1935).
2. Limburgite, Sukumozuka, Shitori-mura, Kume-gun, Okayama Prefecture (HARUMOTO, 1951).
3. Limburgite (grey coloured), Sukumozuka, New Analysis.
4. Limburgite, Ôgusoyama, Shimo-imamyo, Ino-mura, Naka-gun, Shimane Prefecture (WASHINGTON, 1917; TOMITA, 1935).

Table 3. Optical properties of main constituent minerals of basic and ultrabasic inclusions in the olivine basalt from Shimo-ganya, Dögo, Oki Islands

Rock type	Constituent minerals			
	Olivine	Bronzite	Augite	Plagioclase
Wehrlite	$\beta=1.670$ $2V_\gamma=88°$, 90°, 92°	none	$2V_\gamma=50°$ (core), 54° (margin) with exsolution lamellae of bronzite ($2V_\alpha=80°$)	none or rare
Harzburgite	$\beta=1.675$ $2V_\gamma=90°$	$2V_\alpha=85°$, 80°, 75°	none	none
Websterite	none	strained, enclosed in augite	$2V_\gamma=48°$, 50°	none
Bronzitite	none	$2V_\alpha=83°$, 80° with exsolution lamellae of diopside	none	none
Olivine gabbro	$\beta=1.705$ $2V_\alpha=88°$	none	none	$n_1=1.563$ An_{65}
Augite olivine gabbaro	$\beta=1.708$ $2V_\alpha=85°$ rounded grains often enclosed poikilitically in plagioclase	rare	$2V_\gamma=48°$ with exsolution lamellae of bronzite	$n_1=1.560$ An_{60}

lamellae parallel to (100) is rarely observed.

Augite in these inclusions is unhedral, greenish to light brownish in colour in thin section probably containing considerable amounts of Al with fine exsolution lamellae of bronzite.

Bronzite is of Bushveld type with fine exsolution lamellae of diopside. Both

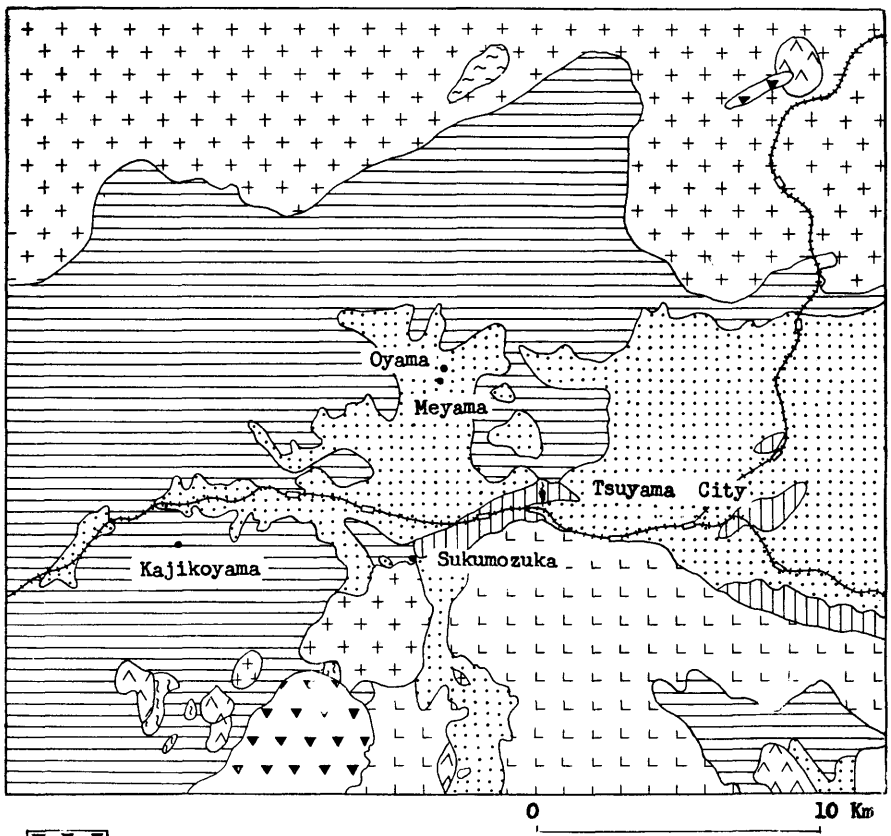

Fig. 2. Geologic map around Tsuyama City, Okayama Prefecture

augite and bronzite are often strained to show wavy extinction.

Plagioclase is bytownite which occurs rarely in peridotitic inclusion interstitially among the olivine and pyroxene grains, and is labradorite in olivine gabbro or augite olivine gabbro. The mineralogical composition and the optical properties of each of these rock type vary gradually from one type to another as can be seen in Tables 1 and 3.

3. Oyama and Meyama, Northwest of Tsuyama City, Okayama Prefecture

Distribution of limburgitic basaltic rocks in the neighbourhood of Tsuyama City, Okayama Prefecture is shown in Fig. 2.

Oyama and Meyama, two small hills, about 7 kilometres northwest of Tsuyama City are constructed of limburgitic basalt, the former is a flow which rests directly on the Tertiary formation (alternation of sandstone and shale) and the latter is a neck intruded into the Tertiary formation. A sketch of the occurrence of the limburgitic basalt of Meyama is shown in Fig. 3.

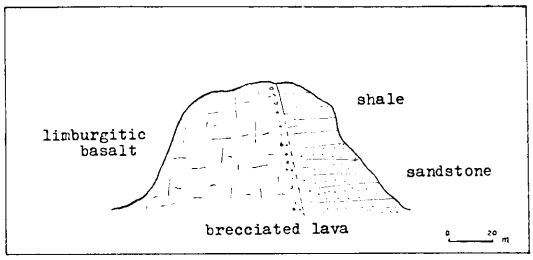

Fig. 3. Sketch of occurrence of limburgitic basalt of Meyama, Okayama Prefecture

These limburgitic basalts, black or grey black in colour, contain abundant olivine and clino-pyroxene phenocrysts. The phenocrysts of olivine are subhedral or unhedral and unzoned, sometimes mosaic in structure exhibiting wavy extinction. Phenocrysts of clinopyroxene are strongly zoned from the core of nearly colourless diopsidic augite to purple rim of titaniferous or aluminous augite.

The groundmass is composed of small amounts of olivine, abundant clinopyroxene, magnetite, ilmenite, biotite, plagioclase, zeolite like mineral and apatite. The presence of highly acicular apatite, ilmenite and biotite is the characteristic feature of these rocks.

Ultrabasic rocks included in these rocks are essentially of peridotite of wehrlite composition composed of coarse grains of olivine, green clino-pyroxene (Cr-diopside) and brown picotite (Table 1). Olivine is unhedral, unzoned, showing translation lamellae. Chrome-diopsides (green in thick section) which occur around the margin of olivine grains or interstitially in the olivine grains are often surrounded by aggregates of fine grains of augite. The aggregates of these fine augite grains are probably the decomposition product derived from the chrome-diopside remaining in their core, after the heat effect of the basalt magma.

4. Sukumozuka and Kajikoyama, West of Tsuyama City, Okayama Prefecture

Small cones at Sukumozuka and Kajikoyama are composed of limburgite lavas which rest on the basement of Sangun metamorphic rocks, granite, and Tertiary formation (Fig. 2). The Sangun metamorphic rocks in this area are composed of sericite quartz schist (sandstone origin) and green schist, intercalating in places lenticular small masses of limestone and intruded by serpentinite.

Limburgite from Sukumozuka has been described briefly by HARUMOTO (1951). The rocks both from Sukumozuka and Kajikoyama are porphyritic composed of phenocryst of olivine and groundmass of olivine, clino-pyroxene, magnetite, very small amounts of sodic plagioclase and nepheline. The chemical composition of the rocks is given in Table 2. Since it contains fairly large amount of nepheline molecule in the norm, the feldspathoid minerals beside the sodic plagioclase, occurring interstitially in the groundmass has been taken as nepheline.

Ultrabasic rocks enclosed in this rock are essentially of dunites composed of coarse grains of olivines (up to 5 mm in maximum diameter) and picotite. The olivines are usually strained with wavy extinction or banded with translation lamellae. Beside this inclusion, single crystal of glomeroporphyritic habit of clino-pyroxene occurs frequently in the rock. The mineral is generally euhedral or subhedral in crystal outline, but sometimes irregularly shaped in which the central part of the crystal is spongy with many pores. The central part of this clinopyroxene is probably the xenocryst decomposed by the magmatic effect and the rim may have grown by the reaction of clinopyroxene xenocryst

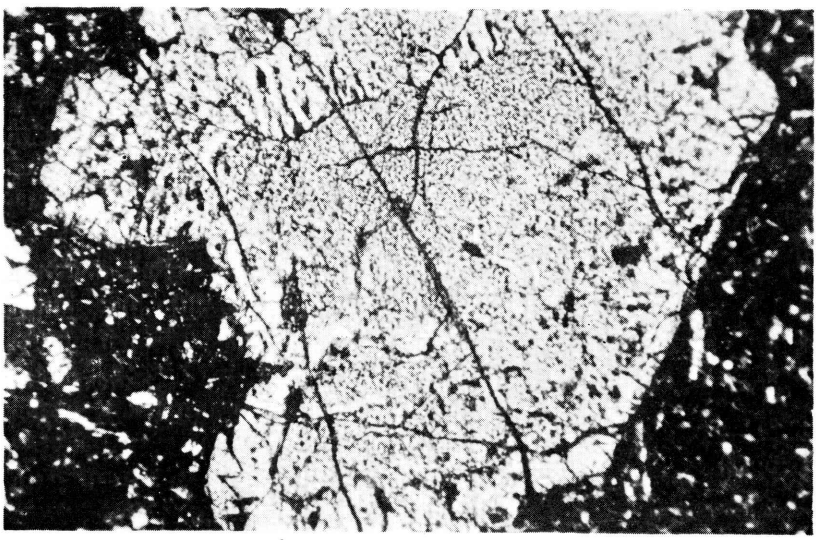

Fig. 4. Spongy augite phenocryst (xenocryst) in limburgite from Sukumozuka, Okayama Prefecture (crossed Nicols)

with the limburgite liquid (Fig. 4).

5. *Nochi and Its Environs, in the Westernmost Part of Okayama Prefecture*

Several cones and flows of basalt and picritic basalt are found around Nochi, at the western extremity of Okayama Prefecture .

The basement rocks of this area are variable, constructed of Palaeozoic,

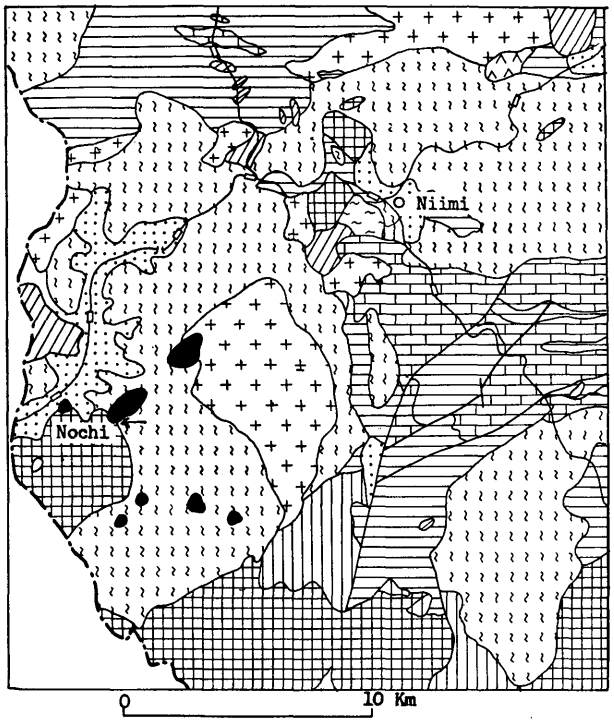

Basalt and picrite basalt
Shale, sandstone and conglomerate
} Neogene Tertiary

Quartz porphyry
Late Mesozoic

Quartz diorite
Biotite granite
Porphyrite
Shale, sandstone and conglomerate
} Mesozoic

Peridotite and serpentinite
Limestone
Slate, sandstone, conglomerate, basalt flow and tuff
} Palaeozoic

Locality of sample (No. Kb 11a)

Fig. 5. Geologic map around Nochi in the westernmost part of Okayama Prefecture

Mesozoic and Tertiary sedimentary and igneous rocks, on which occur many basaltic cones. The distribution of these basaltic rocks is shown in a geological map (Fig. 5).

Ultrabasic rocks included in these basalts are in most part of harzburgite and websterite compositoins (Table 1).

The harzburgite is composed of coarse grains of olivine and bronzite. Those of olivine are generally rounded and strained showing wavy extinction, and enclosed in the Bushveld type bronzite crystals.

Websterite, the most abundant type of inclusion found in this basalt, is composed of diopsidic augite and bronzite. Chemical compositions of these two minerals and the estimated bulk composition of websterite are given in Table 4.

Table 4. Chemical composition of aluminian bronzite and aluminian diopsidic augite of websterite inclusion, and estimated bulk composition of the websterite, in the basalt from Nochi, in the westernmost part of Okayama Prefecture

Wt. per cent.	A	B	C	Number of atoms on the basis of 6 oxygens	A	
SiO_2	51.26	48.66	48.26	Si^{4+}	1.814	2.000
TiO_2	0.38	0.83	0.80	Al^{3+}	0.186	
Al_2O_3	6.36	8.84	8.62	Al^{3+}	0.079	2.019
Fe_2O_3	2.48	2.74	2.70	Ti^{4+}	0.010	
FeO	8.12	5.32	5.90	Fe^{3+}	0.066	
MnO	0.18	0.14	0.14	Fe^{2+}	0.240	
MgO	27.88	15.77	16.20	Mn^{2+}	0.005	
CaO	3.49	16.85	16.01	Mg^{2+}	1.469	
Na_2O	0.26	1.13	1.07	Ca^{2+}	0.132	
K_2O	tr.	tr.	tr.	Na^{1+}	0.018	
H_2O (+)	0.15	0.29	0.28	K^{1+}	tr.	
H_2O (−)	0.00	0.00	0.00			
P_2O_5	n.d.	0.02	0.02	Atomic ratio		
Total	100.56	100.59	100.00	Ca	7.2	
Analyst	T. KATSURA	T. KATSURA	Calculated (A×5 B×95)	Mg	79.8	
				Fe	13.0	

A: Aluminian bronzite including exsolution lamellae of diposide
B: Aluminian diopsidic augite including exsolution lamellae of augite and pigeonite
C: Estimated bulk composition of websterite inclusion

The augite, pitch-black under the naked eye, and light brown in thin section, could hardly be recognized as diopsidic without the chemical analysis. Since the mineral contains a large amount of Al ions, it may be called as aluminian (diopsidic) augite. It is also characterized by the presence of very complicated exsolution lamellae constructed of augite and pigeonite, the details of which will be given in later chapter. Bronzite contains also higher amount of Al ions, which have probably reflected to the colour of pleochroism varying from brownish to light yellowish brown in thin section.

Both augite and bronzite have been changed at the margin of the inclusion to pyroxenes of certain textures. Bronzite has changed to aggregate of pigeonite

or augite and olivine grains (pseudo-hypersthene of TOMITA, 1932). Augite has partly remelted, producing drop like or worm shaped pores, and resembles in it texture a vitrified plagioclase xenocryst. The pores of augite are filled with fine particles of iron ores, or serpentine and feldspathic minerals. The texture is temporarily called spongy texture in this paper.

The vitrification or the decomposition of these pyroxenes is confined at the margin of the nodule with the depth of about 0.4-0.8 milimetres which indicates the limit of magmatic effect. The central part of this crystal is unaffected.

Beside this inclusion, crystals of augite with spongy texture on the entire crystal and pseudo-hypersthene are often met with as scattered phenocrysts. They are obviously the xenocrysts mechanically disintegrated from the peridotitic inclusion.

6. Ôgusoyama, Shimane Prefecture

Ôgusoyama, a small hill (250 metres high) about 14 kilometres SSE of Hamada City in the western part of Shimane Prefecture, has been known long by the occurrence of limburgite.

The limburgite mass with the apparent thickness of about 60 metres from the base to the top of the cone, rest on the boundary of medium-grained biotite hornblende granodiorite and Palaeozoic formation, the latter is composed of biotite hornfels and biotite semischist (Fig. 6).

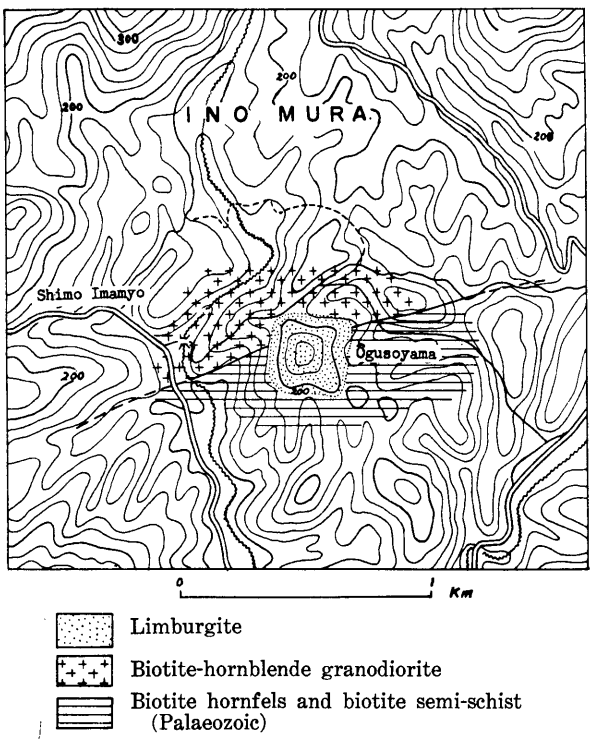

Fig. 6. Geologic map of Ôguso-yama, Shimane Prefecture

TOMITA (1932) has described the optical constants of the constituent minerals of this rock, in which he distinguished two rock types; the one is a common limburgite composed of olivine, titan-augite and colourless glass, and the other contains labradorite in the groundmass together with olivine, titan-augite and brown glass. He divided olivine phenocrysts of both rock types into 3 groups with regard to the difference of index of refraction, of which the one type of olivine was assumed by him to be a xenocryst.

Owing to the unfavourable exposure of the area, the structure of the cone, and hence the relation of two rock types as Tomita mentioned could not be clarified.

The age of limburgite eruption is not clearly known. I have collected several granodiorite blocks in many blocks of olivine rich nodules at the top of the hill. The granodiorite of these blocks is quite the same in its mineralogical composition and texture as the rock which constructs the basement of the limburgite lava. Accessory zircons from both of these granodiorites have been separated and examined. The mass colour of zircons separated from the blocks was dull brownish red, while that of basement granodiorite was grey. If the blocks in question were the xenoliths or the ejectas of the limburgite eruption, and if the Tomita's zircon correlation method is accepted (TOMITA, 1954), the age of limburgite eruption may be referred, according to the colour of zircon in the granodiorite blocks, to Upper Miocene.

The limburgite is grey or black, compact and porphyritic with a large amount of olivine and less abundant clino-pyroxene as phenocrysts and a large amount of olivine and augite, together with lesser amounts of magnetite, ilmenite, apatite and glass with or without sodic plagioclase in the groundmass.

The limburgite encloses abundant olivine rich inclusions, the diameter of which often reaches to about 10 centimetres in diameter. I have collected about one hundred specimens of inclusions mostly of blocks at the top of the hill, in which the rocks with the mineral composition of dunite or peridotite were the most abundant. The rock types and the frequency of these inclusions have been given in Table 1.

Olivine, occurring as coarse grains in these peridotitic rocks, is more strongly strained than that in any other inclusions from other places so far as I have examined, and exhibits fine translation lamellae and wavy extinction. Typical examples of most strained olivine are illustrated on Plate 25.

Bronzite, chromian diopside and augite are also strained showing wavy extinction. Chromian diopside, emerald green in colour, occurs interstitially among the olivine grains but is sometimes rounded, being enclosed in the olivine crystals.

Each constituent mineral of these inclusions has been affected at the margin by the magma, i.e. the olivine has changed to fine mosaic aggregate, and sometimes to iddingsite, the bronzite decomposed to pseudo-hypersthene, and the augite shows a spongy texture. The constituents of these rocks have also been separated into the limburgite as xenocrysts.

7. Kurose, at the Mouth of Hakata Bay, Fukuoka City

Kurose (Black Rock), a rock at the Mouth of Hakata Bay near Genkai Islet is alkaline olivine basalt composed of phenocrysts of olivine (Fa 15-20) and augite in the groundmass of olivine, augite, plagioclase, alkali-feldspar, magnetite, hematite, chloritic mineral and glass.

Peridotitic rocks included in this basalt, several centimetres in diameter are of wehrlite and harzburgite (Table 1), composed of olivine, augite and picotite, or olivine, bronzite and picotite respectively.

Olivine in these rocks is strained with translation lamellae, the contact with the basalt has been changed to bowlingite. Bronzite is often decomposed to aggregate of olivine and pigeonite in the contact with the host rock.

Most phenocrysts of olivine and augite in this basalt are also regarded as xenocryst derived from these peridotitic rocks. Of these, some olivine phenocrysts are zoned consisting of strained core (with translation lamellae) and successive outer zones of bowlingite and clear olivine, of which the latter has probably been grown around bowlingite (Fig. 7). Phenocrysts of augite often show spongy texture. In some other cases, the mineral enclose olivine grains together with some amount of intermediate plagioclase as is shown in Fig. 8.

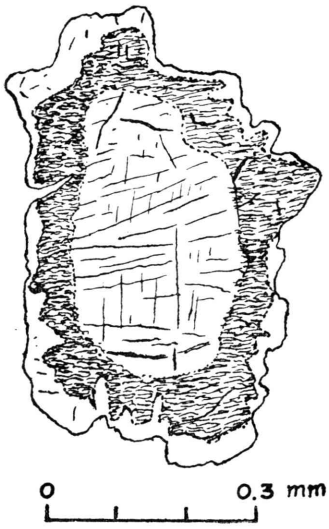

Fig. 7. Zoned olivine consisting of strained core and successive outer zones of bowlingite and clear olivine; xenocryst separated from peridotitic inclusion in alkaline olivine basalt from Kurose, near Genkai Islet at the mouth of Hakata Bay

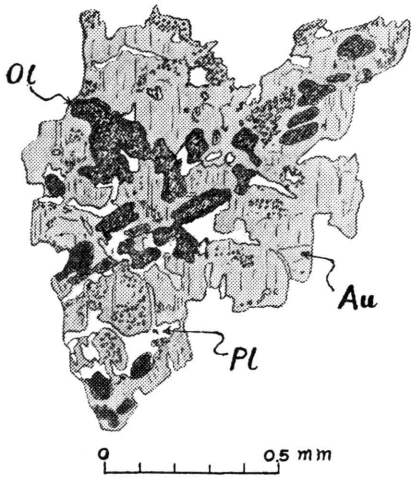

Fig. 8. Decomposed augite xenocryst (Au) enclosing olivine (Ol) and plagioclase (Pl)

8. Takashima Islet and other places in the Karatsu Area, Saga Prefecture

The largest group of specimens among the ultrabasic inclusions of various localities described in this paper has been collected from the basalts distributed

around Karatsu City, Saga Prefecture, northern Kyushu.

Previously, AOYAMA (1942) has given a brief note on the occurrence of olivine and pyroxene nodules from Takashima Islet, in the Bay of Karatsu with chemical analyses of olivine and aluminous pyroxene in each nodule. KOBAYASHI and others (1955, 1956) and AOKI (1959) have also made a short description about the nodules distributed at several places around the Karatsu City, but systematic petrographic study of these rocks has never been presented.

(a) Occurrence of basaltic rocks and its inclusion.—Basaltic rocks distributed in this area, including Karatsu, Yobuko, Imari and Sasebo areas, are distinguished into several stages of eruptions associating with andesites, trachytes and rhyolites, all of which rest on the flat errosion surface (peneplain) of granites and Tertiary sediments. The district has been noted petrologically, as the 'mixed province' (TOMITA, 1935, 1958) of several rock types of alkaline and calc-alkaline volcanic rocks. The generalized sequence of volcanic rocks from this area is shown in Table 5.

Table 5. Generalized sequence of volcanic rocks in the Karatsu area

Clay, sand and gravel	Alluvium
Grey olivine basalt	Diluvium?
Trachyte and trachyandesite	
Riebeckite trachyte	
Acicular plagioclase bearing basalt	Probably Pliocene
Augite olivine basalt	
Porphyritic and non porphyritic olivine basalt	..Contains basic and ultrabasic inclusions
Peneplain	
Miocene sandstone, mudstone and siltstone with oliv. dolerite intrusive	Biotite granite and hornblende-biotite granodiorite

Of several lava flows of the Karatsu area, the lower-most basalt flow, which is most widely distributed, contains abundant peridotitic and gabbroic inclusions. I have collected more than one hundred rock specimens of large inclusions from this area. They are collected mainly at Takashima Islet in the Bay of Karatsu, and at Hinode-matsu, Iwano and its neighbours, west of Karatsu City. The distribution of these inclusions is shown in Fig. 9.

The main part of the basalt in question is dark grey to grey, compact, nearly non-porphyritic olivine-basalt with maximum thickness of about 40 metres. The rock is, however often variable in facies as it contains platy plagioclase at

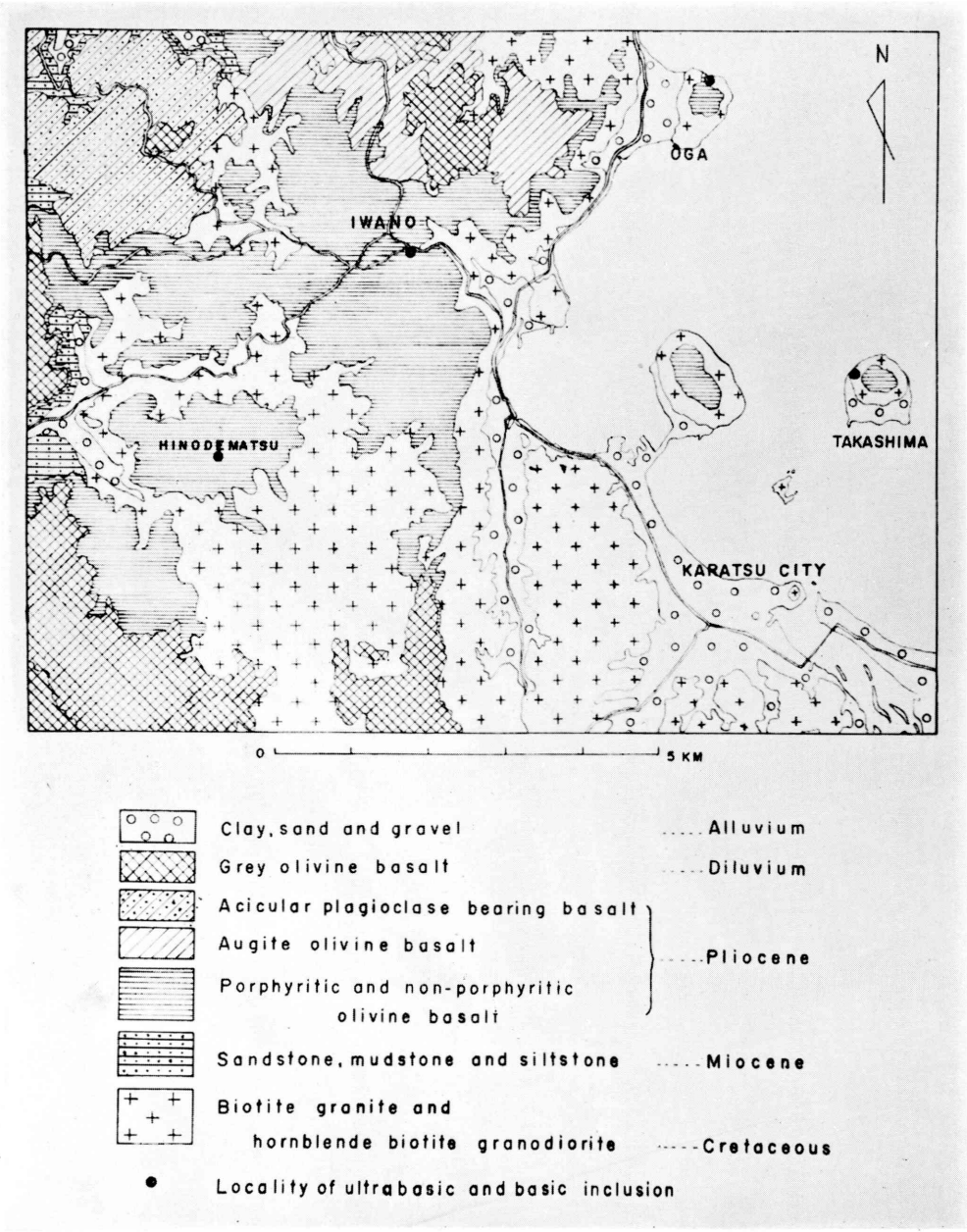

Fig. 9. Geologic map around the Karatsu area, Saga Prefecure

the base of the flow or at the margin of the neck (at Ôga), and most strongly porphyritic where inclusions are abundant, since the mechanically disintegrated constituents of peridotitic, gabbroic and granitic inclusions such as olivine, pyroxene, plagioclase and quartz are scattered as xenocrysts.

Distribution of inclusions in the lava is uneven, and regular arrangements of these rocks were not found in any of these basaltic rocks. On the contrary,

abundant ultrabasic rocks and a few granitic rocks enclosed in the basalt tend to increase in a vent or in a dyke, and decrease in number down to the margin of the flow. Thus, dyke of basalt at Ôga contains fairly large number of granitic and ultrabasic inclusions.

At Takashima Islet, thick bed of basaltic agglomerate and the basalt flow at the top, which rest on the granite foundation, contain abundantly many kinds of ultrabasic rocks. At the mesa constructed of basalt around Hinode-matsu, inclusions of ultrabasic rocks are scarcely found near the base of the flow, but are concentrated in a certain place of the flow.

There is a general tendency that many xenolithic rock fragments tend to occur abundantly in a dyke or in a volcanic vent, and decrease in their amount as they are apart from the vent. This has been recognized by many authors (SMITHE, 1914, etc.). From my own field experience, granitic xenoliths in basalt are most abundant in the vent or in the neck than in its flow. A typical example containing most abundantly various kinds of xenoliths and nodules in the vent of two-pyroxene andesite has been shown in my previous paper (YAMAGUCHI, 1961b).

If this general tendency is accepted, concentrated occurrence of ultrabasic inclusions in certain places in this area may indicate that each of these places can approximately be regarded as the centre of eruption, even if it has not been confirmed directly by a field work. In other words, the basalt containing ultrabasic inclusions at several local places in this area should be composite, which erupted from several centers.

The age of eruption of the basalt containing the inclusions in question is not clearly known. TOMITA (1951) correlated the peneplain at the base of the flow to that of Kissyu and Meisen district, north Korea, or that of lower level peneplain recognized on Chugoku district Southwest Japan. On the other hand, the peneplain of granite is widely developed in the area of Setouchi Inland Sea which is directly covered by basalts and allied sanukitic rocks. The age of this peneplanation is regarded, based on my field study of Shodoshima Island (YAMAGUCHI, 1958), as lower Pliocene.

On this evidence and for the reason of the volcanostratigraphical and petrographical similarity of the rocks to those of the Setouchi Inland Sea area, the basalts of the Karatsu area together with allied sanukitic rocks may be regarded as eruptions of a Pliocene age.

(b) Description of Ultrabasic Inclusion.—Ultrabasic inclusions collected from this area are variable in rock type, shape and size. They are mostly angular or subangular, and reach to 20 centimetres in maximum diameter.

The rock types of ultrabasic inclusions are divided into four groups, which are shown in Table 1 together with constituent minerals and the frequency. Their macroscopic and microscopic features are illustrated on Plates 24-25; description of each rock type follows.

(i) Dunite Inclusion—The rock is found abundantly as inclusions in the basalts from Takashima Islet and Hinodematsu. They are rounded or subangular

in shape, light green or light yellowish green in the fresh samples, but are yellow brown or reddish brown in the oxidized and decomposed samples. The rock is composed of mosaic aggregates of coarse grains of olivine, with the maximum diameters of about 1 centimetre, and picotite; the interstices of these minerals are filled up with thin films of serpentine.

Olivine is generally very transparent and homogenous and almost free from inclusions, except of picotite grains, in the main part of the rock, but is slightly zoned at the rim of the crystal in contact with the host rock. Banded structure due to the translation lamellae in the olivine crystal is the general feature of the rock (Plate 4). The olivine is mosaic in crystal outline both in the core and at the margin of the rock. It is coarse (about one centimetre) and Mg rich in composition (Fa 10-15) in the core, while medium grained (0.2-0.8 milimetres) and slightly Fe richer in composition (Fa 20) at the margin.

Flow lines are sometimes recognized in the basalt host around the margin of the inclusion.

(ii) Peridotite Inclusion—The rock, angular or subangular, is composed mainly of olivine and green diopsidic augite, with subordinate amounts of bronzite, picotite and with or without a little amounts of calcite (Table 6). Some specimens from Hinodematsu show layering by the alternation of larger and smaller amount of green diopside contained in the rocks (Plate 24, No. 11).

Table 6. Modes of peridotite inclusions in basalt from Takashima Islet, Karatsu City, Saga Prefecture

Wt. per cent.	A	B
Olivine	95.5	94.8
Picotite	2.5	2.3
Green diopsidic augite	3.0	2.0
Bronzite and others	none	0.9

Two types of olivine have been recognized, the one is a medium rounded grains (0.5-0.8 mm in diameter, $2V_\gamma = 82°$-$86°$) with no translation lamellae and included in the augite crystals, and the other is a larger mosaic grains (2 mm in diameter, $2V_\gamma = 90° \pm$) with distinct translation lamellae.

Both diopsidic augite and bronzite are coarse-grained (0.1-10 mm) with distinct exsolution lamellae and often showing undulose extinction. The diopsidic augite often includes ilmenite like crystals of slender habit. The minerals are corroded at the margin with the basalt magma, and often decomposed to show a spongy texture associated with olivine ($2V_\gamma = 98°$), alkali-feldspar, and brown glass.

(iii) Diallagite and Websterite Inclusions—The rock with maximum diameter of about 20 centimetres is angular or subangular in shape, coarse grained, composed of augite and picotite, with or without some amounts of olivine or bronzite and plagioclase. An augite, pitch black in hand specimen, is revealed by the chemical analysis as a high alumina variety (aluminian diopsidic augite,

Tables 7 and 8, No. 1). The mineral is unhedral and strongly strained with translation lamellae (parallel to 001) or wavy extinction. It is also characterized by the very complicate exsolution lamellae. The mineral is spongy at the margin of the nodule with inclusions of glass and iron ores. The spongy augite, probably formed by the heat effect of basalt magma, is slightly more diopsidic than the core (Tables 7 and 8, No. 2-A, 2-B).

(iv) Gabbroic Inclusion—The rock is composed generally of coarse grains of aluminus augite, bronzite, plagioclase and drak green spinel with or without small amounts of olivine or serpentine. The aluminus augite is mosaic (0.2-1.5 mm in diameter, $2V_\gamma=57°$–$56°$) and often strained. Small mosaic grains are often zoned with calcic core ($2V_\gamma=57°$) and ferous margin ($2V_\gamma=50°$). Bronzite (6 mm± in diameter) is also mosaic, and pleochroic ($2V_\alpha=80°$–$78°$), containing exsolution lamellae of diopside. Plagioclase is bytownite and often strained, showing banded structure. It is also characterized by the presence of complex twinning of albite and Pericline law, and of lamellae composed probably of calcic ($2V_\alpha=78°$) and sodic ($2V_\alpha=90°$) bytownites. Dark green spinel (hercynite?) occurs as rounded grains (0.1–1 mm) interstitially in the augite grains or in the contact of plagioclase and augite.

II. Physical and Chemical Properties of Constituent Minerals of Ultrabasic Inclusions and Allied Materials

1. Separation of Samples

The samples used in this study were first separated by hand picking. They were powdered, silk screened (150-200 mesh) and passed repeatedly through the Frantz isodynamic separator. Impurities of serpentine and spinel present in small amount were removed with methylene iodyde and or crelici solution. The pyroxene residues were often treated for several minutes with dilute hydrochloric acid and or hydrofloric acid. In the case of olivine residues, the iddingsite impurities were often treated by dilute hydrofloric acid.

2. Chemical Composition and Optical Properties of Clinopyroxenes

Table 7 and 8 record new data of chemical compositions and optical properties of clinopyroxenes which were separated from ultrabasic inclusions, together with data by previous authors of those from basalts and gabbro; the identical material of the latter has been newly measured by the X-ray method. The locality and brief note of each sample are given in the next section.

3. Sources of Data on Clinopyroxenes

(Unit cell volume and packing index are obtained for No. 1-No. 30 from chemical analyses and X-ray determination and for No. 34-No. 71 from chemical analyses and specific gravities).

1. Aluminian diopsidic augite of diallagite inclusion in basalt from Takashima Islet, in the Bay of Karatsu, Saga Prefecture, Japan (Sample No. TK01-2, new analysis).

2A. Aluminian diopsidic augite, rim of No. 1, with spongy texture. Contains inclusions of glass and iron ores (Sample No. TK 01-4, new analysis).
2B. Same as No. 2A. Corrected about 5 per cent of glass and iron ore impurities.
3. Aluminian diopsidic augite of websterite inclusion in basalt from Nochi, west in Okayama Prefecture, Japan (Sample No. Kb 11a-1, new analysis).
4. Rim of No. 3, with spongy texture. Contains inclusions of glass and iron ores (Sample No. Kb 11a-2, new analysis).
5. Chrome diopside in peridotite from Horoman, Hokkaido (Sample No. 86, refer YAMAGUCHI, 1961a).
6. Chrome diopside of chromite vein in dunite from Higashi-Akaishi, Shikoku (Sample No. AK46. Recalculated composition. Refer HARADA, 1943 and YAMAGUCHI, 1961a).
7. Chromian diopside, phenocryst in basalt from Sano, Yamanashi Prefecture, Japan. Chemical analysis and optical properties were quoted from KUNO (1957). Identical material from the same locality collected by late Sokichi Koo are used for the determination of cell dimensions.
8. Augite, black type, phenocryst in basalt tuff breccia from Nishiga-také, Saga Prefecture, Japan. The mineral is often enclosed in green type augite. Chemical analysis and optical properties were quoted from MIYAKE (1948). Identical material collected from the same locality are used for the X-ray analysis.
9. Augite, green type, phenocryst in basalt and basalt tuff breccia from Nishiga-také, Saga Prefecture, Japan. The mineral occur around the black type (No. 8) augite. Quoted from MIYAKE (1948). Identical material collected from the same locality are used for the X-ray analysis.
10. Augite in basalt from Uyama-misaki near Hagi, Yamaguchi Prefecture, Japan. Chemical composition and optical properties were quoted from SUGI (1942). The same material separated by SUGI were refined and used for X-ray analysis.
11. Augite in basalt from Kuchinotsu, Nagasaki Prefecture, Japan. Quoted from SUGI (1951b). The same material separated by SUGI were refined and used for X-ray analysis.
12. Purple augite in dolerite from Takakusayama, Shizuoka Prefecture. Quoted from SUGI (1951a). The same material were used for X-ray analysis.
13. Diallage in gabbro from Ayabe, Kyoto Prefecture. Quoted from SUGI (1951a). The same material were used for X-ray analysis.
14. Augite from gabbro-picrite, 4526, Skaergaard intrusion, East Greenland (BROWN, 1957, 1960).
15. Augite from lower olivine gabbro, 4392, Skaergaard intrusion (BROWN, 1957, 1960).
16. Augite from lower olivine gabbro, EG. 4389, Skaergaard intrusion (BROWN, 1960, No. 3).
17. Augite from middle gabbro, 4369, Skaergaard intrusion (BROWN, 1957, 1960).
18. Augite from middle gabbro, 4341, Skaergaard intrusion (BROWN, 1957, 1960).
19. Augite from ferrogabbro, 4430, Skaergaard intrusion (BROWN, 1957, 1960).
20. Augite from ferrogabbro, 4306, Skaergaard intrusion (BROWN, 1957, 1960).
21. Augite from ferrogabbro, 4309, Skaergaard intrusion (BROWN, 1957, 1960).
22. Augite from ferrogabbro, 4314, Skaergaard intrusion (BROWN, 1957, 1960).
23. Ferroaugite from ferrogabbro, E.G. 4318, Skaergaard intrusion (BROWN, 1960, No. 10).
24. Ferrohedenbergite from transgressive granophyre sill, E.G. 4489, Skaergaard intrusion (BROWN, 1960, No. 11).
25. Augite from layered ultrabasic rocks of Rhum, Inner Hebrides (BROWN, 1960, No. A).
26. Salite in olivine eucrite (HK 33010901e) from ejected block in basalt tuff, Taga Volcano, Japan (KUNO, 1955, No. 1).
27. Augite, phenocryst in hypersthene-olivine-augite andesite (HK 35090603) of Hakone Volcano, Japan (KUNO, 1955, No. 5).
28. Diopside in skarn rock, Brunner Hill magnetite deposit near Colton, Stork Quadrangle, St. Lawrence Co., N.Y. Specimen No. BH 1.23 (HESS 1949, Analysis 35; Kuno and HESS 1953, No. 4). The value of packing indices in parentheses is calculated from specific

gravity and chemical composition.

29. Ferrosalite from marble layer in Whiteface anorthosite, Adirondacks, N.Y. Pokamoonshine Quarry, Ausable Quadrangle. Specimen No. 1197a (HESS 1949, Analysis 16; KUNO and HESS 1953, No. 5).
30. Hedenbergite, Herault, California. Specimen No. HER (HESS 1949, Analysis 18).
31. Stillwater clinopyroxene. No. EB 175 (HESS 1960).
32. Stillwater clinopyroxene. No. EB 41 (HESS 1960).
33. Bushveld clinopyroxene. No. 7493 (HESS 1960).
34. Chromian diopside from 'olivine bomb' (peridotitic) in basaltic tuff, Kapfenstein, Styria, Austria (ROSS et al., 1954, No. 5).
35. Chromian diopside from nodule in olivine basalt, Ludlow, San Bernandino County, California (ROSS et al., 1954, No. 2).
36. Chromian diopside from nodule in volcanic bomb, Camargo, Chihuahua, Mexico (ROSS et al., 1954, No. 1).
37. Chromian diopside from olivine bomb in the tuff of cinder cone of scoriaceous basalt, Peridot Cove near Globe, Arizona (ROSS et al., 1954, No. 3).
38. Chromian diopside from nodule in basalt, Salt Lake Crater, Oahu, Hawaiian Islands (ROSS et al., 1954, No. 8).
39. Chromian diopside from nodule in volcanic bomb, Dreiser Weiher, Eifel, Germany (ROSS et al., 1954, No. 4).
40. Chromian diopside from nodules in basalt tuff breccia, Ichinomegata, Akita Prefecture, Japan (ROSS et al., 1954, No. 7).
41. Chromian diopside from nodules in basalt, small cinder cone, Hale Pohaku, south flank of Mauna Kea, Hawaii (ROSS et al., 1954, No. 10).
42. Chromian diopside from nodules in basalt, 1801, Kaupulehu flow, Hualalai, Hawaii (ROSS et al., 1954, No. 11).
43. Chromian diopside from dunite, Webster, North Carolina (ROSS et al., 1954, No. 13).
44. Chromian diopside from dunite, Twin Sisters, northern Whatcom County, Washington (ROSS et at., 1954, No. 12).
45. Chrome diopside from websterite, Webster, North Carolina. Specimen No. WEB (HESS, 1949, Analysis 1).
46. Augite from anorthosite gabbro, Keene Valley road, Elizabethtown quadrangle, N.Y. Specimen No. 6072 (HESS, 1949, Analysis 21).
47. Chrome augite from pegmatitic gabbro below chromite horizon, Stillwater complex, Montana, Specimen No. I 52 (HESS 1949, Analysis 5).
48. Titanaugite from pegmatitic zone in gabbro sill, shore of Lake Superior, Cook Co., Minn· Specimen No. D2 (HESS 1949, Analysis 30).
49. Salite, skarn inclusion in gabbroic anorthosite magma. Lake Placid Quadrangle, N.Y. Specimen No. 6102 (HESS 1949, Analysis 23).
50. Salite from skarn rock, Clifton Mine, magnetite deposit. Specimen No. CN 69.1 (HESS, 1949, Analysis 37).
51. Augite from coarse anorthosite, Mt. Marcy, St. Regis Quadrangle. Specimen No. 5915 (HESS, 1949, Analysis 22).
52. Ferroaugite, inclusion in granoblastic melanocratic augite syenite, Saranac Quadrangle, Adirondacks. Specimen No. 5657a (HESS, 1949, Analysis 17).
53. Augite from mafic gabbro dike in anorthosite, 2 miles S.E. of Gates Corners, Antwerp Quadrangle, Adirondacks. Specimen No. 4015 (HESS, 1949, Analysis 13).
54. Augite from metagabbro; garnet-augite-oligoclase-granulite, dike one mile west of Elizabethville, N.Y. Specimen No. 5641b (HESS, 1949, Analysis 14).
55. Augite from medium grained granite gneiss. Found as the predominant rock type in the Lima Quarry. A part of the Lima granite gneiss, Piedmont Province, Pennsylvania and Delaware (NORTON and CLAVAN, 1959, 35-24N).
56. Augite from fine-grained massive gabbro, dikes intrusive into quartz-diorite. Alapocas Quarry, Brandywine Creek, Wilmington, Delaware (NORTON and CLAVAN, 1959, 35-9N).

57. Augite from medium fine-grained hornblende norite showing faint foliation. North of Tallyville, Wilmington, Delaware (NORTON and CLAAN, 1959, 35-5N).
58. Augite from fine grained quartz-diorite showing faint gneissic banding. Occur as a xenolith in the Lima granite gneiss (NORTON and CLAVAN, 1959, 35-25N).
59. Augite from medium grained massive quartz norite. Franklin and Sycamore Streets, Wilmington, Delaware (NORTON and CLAVAN, 1959, 35-6N).
60. Augite from fine grained quartz diorite. Alapocas Quarry on the east bank of Brandywine Creek in Wilmington, Delaware (NORTON and CLAVAN, 1959, 35-8N).
61. Diopside from fine-grained massive gabbro xenolith in granite-gneiss, north of Upper Bridge, Crum Creek Reservoir (NORTON and CLAVAN, 1959, 35-1N).
62. Augite from medium grained hypersthene diorite. Radnor Quarry, Baltimore gneiss (NORTON and CLAVAN, 1959, 35-13N).
63. Augite from coarse grained hornblende-eucrite, south side of Faulk Road, 1.5 miles northeast of the intersection of U.S. Route 202 (NORTON and CLAVAN, 1959, 35-19N).
64. Augite from coarse grained eucritic norite. Part of an ultrabasic intrusion into Wissahickon formation. West Chester Pike at the Dinwoody Home (NORTON and CLAVAN, 1959, 35-32N).
65. Clinopyroxene from peridotite xenolith in a thin basalt flow at the Drogheda Trigonometrical Survey Station, about 15 miles southeast of Oberon, New South Wales (WILSHIRE and BINNS, 1961, Table 4a, No. 2).
66. Clinopyroxene from xenocryst in the lamprophyre sill, 2 to 3 ft thick intruded into Permo-Carboniferous sandstone at Nanedewar Mountain, New South Wales (WILSHIRE and BINNS, 1961, Table 4a, No. 3).
67. Clinopyroxene from peridotite xenolith in basalt dyke, 2 miles south of Kiama, New South Wales (WILSHIRE and BINNS, 1961, Table 4a, No. 1).
68. Clinopyroxene from pyroxenite xenolith in monchiquite dykes exposed in Bombo Quarry, 1 mile north of Kiama, New South Wales (WILSHIRE and BINNS, 1961, Table 4a. No. 4).
69. Clinopyroxene from gabbro xenolith in monchiquite dykes at Bombo Quarry, 1 mile north of Kiama (WILSHIRE and Binns, 1961, Table 4a, No. 6).
70. Clinopyroxene from pyroxenite phase of the Mount Dromedary laccolith (WILSHIRE and BINNS 1961, Table 4a, No. 8).
71. Clinopyroxene from pyroxenite xenolith in monchiquite dyke at Bombo Quarry, 1 mile north of Kiama, New South Wales (WILSHIRE and BINNS, 1961, Table 4a, No. 5).

4. The Exsolution Lamellae of Clinopyroxenes

Pyroxenes in plutonic rocks often contain blebs or lamellae of different pyroxenes or other opaque minerals. The well known "schiller inclusion" in "bronzite", the name in the original sense, is one of the typical examples.

The orthopyroxene of Bushveld type (HESS and PHILLIPS, 1938) or the orthopyroxene with oriented plate of augite (POLDERVAART, 1947; WALKER and POLDERVAART, 1949) which has peculiar laminated structure or graphic intergrowth of diopside and orthopyroxene (host) has been considered as the result of exsolution.

The similar exsolution pattern in augite with pigeonite or hypersthene has also been reported by HESS and HENDERSON (1949), MORIMOTO and ITO (1958) and BROWN (1957).

The careful observation of both orth- and clino-pyroxenes in dunite of Hokkaido, olivine and pyroxene rich inclusions in limburgites and basaltic rocks from southwest Japan has revealed that the laminated structures or the oriented inclusions of pyroxenes are of rather wide occurrence. As the exsolution pattern,

Table 7. Chemical compositions and optical properties

Wt. per cent \ Sample No.	1	2-A	2-B	3	5	6
SiO_2	47.67	53.87	52.62	48.66	50.67	53.32
TiO_2	1.10	0.89	1.06	0.83	0.48	n.d.
Al_2O_3	8.21	9.25	8.39	8.84	4.84	3.70
Fe_2O_3	3.73	2.41	2.89	2.74	0.91	1.15
Cr_2O_3	n.d.	n.d.	n.d.	n.d.	1.46	1.06
FeO	5.74	3.69	4.42	5.32	1.41	0.23
MnO	0.15	0.14	0.17	0.14	0.10	n.d.
MgO	14.36	10.11	12.13	15.77	17.77	15.40
CaO	18.33	14.06	16.87	16.85	21.16	25.00
Na_2O	0.95	0.97	0.97	1.13	0.82	—
K_2O	0.05	0.16	0.12	tr.	tr.	—
H_2O (+)	0.23	1.70	0.36	0.29	0.38	—
H_2O (−)	0.12	3.02	none	0.00	none	—
P_2O_5	0.02	n.d.	—	0.02	—	—
NiO	n.d.	n.d.	—	n.d.	—	0.14
V_2O_5	n.d.	n.d.	—	n.d.	—	—
Total	100.66	100.27	100.00	100.59	100.00	100.00
Analyst	T. KATSURA	T. KATSURA	Calculated	T. KATSURA	Calculated	Calculated
β	1.695 (mean)	1.700 (mean)	1.700 (mean)	1.696 (mean)	1.687-1.693 (mean) 1.690	1.681-1.685
2V (+)	56°	54°	54°	54°-0°	56°	57° (avg)
Exsolution lamellae	001	none	none	(100) and (001) complex	present but rare	present but rare

Table 8. Ionic contents of aluminian and chromian diopside and augite (on the

Ions \ Sample No.	1	2-A	2-B	3	5	6
Si^{4+}	1.759	1.985	1.903	1.775	1.833	1.930
Al^{3+}	0.357	0.401	0.357	0.380	0.206	0.158
Ti^{4+}	0.031	0.031	0.029	0.023	0.013	n.d.
Fe^{3+}	0.103	0.067	0.079	0.075	0.025	0.031
Cr^{3+}	n.d.	n.d.	n.d.	n.d.	0.042	0.030
Fe^{2+}	0.177	0.114	0.134	0.162	0.043	0.007
Mn^{2+}	0.005	0.004	0.005	0.004	0.003	n.d.
Ni^{2+}	—	—	—	—	—	0.004
Mg^{2+}	0.789	0.555	0.653	0.857	0.958	0.830
Ca^{2+}	0.724	0.555	0.653	0.658	0.820	0.969
Na^{1+}	0.068	0.069	0.068	0.080	0.057	n.d.
K^{1+}	0.002	0.008	0.006	n.d.	tr.	n.d.
OH^{1-}	—	—	—	—	0.092	—
O^{2-}	6.000	6.000	6.000	6.000	5.908	6.000
W cell ($\times 10^{-24}$g)	1475.97	—	1437.37	1458.78	1443.25	1443.62
SG (calc)	3.410	—	3.304	3.367	3.311	3.280

of aluminian and chromian diopside and augite
(materials used for the measurement of cell dimensions)

7	8	9	10	11	12	13
53.42	47.67	50.67	49.71	52.02	48.73	48.46
0.12	1.14	0.56	0.75	1.46	1.82	1.74
0.68	5.10	4.11	8.05	7.90	4.46	4.44
1.36	3.14	1.94	2.56	1.88	2.65	2.32
0.56	0.35	0.62	n.d.	n.d.	n.d.	n.d.
2.01	4.38	3.17	6.10	10.84	6.01	6.60
0.07	0.09	n.d.	n.d.	n.d.	n.d.	n.d.
15.99	16.35	17.13	14.18	13.38	14.50	14.60
25.75	19.15	20.43	17.07	10.16	21.06	21.02
0.12	0.57	0.38	n.d.	n.d.	0.46	0.42
0.06	0.25	0.25	n.d.	n.d.	0.05	0.04
0.16	n.d.	n.d.	n.d.	n.d.	n.d.	n.d.
0.01	0.12	0.06	n.d.	n.d.	n.d.	n.d.
0.03	n.d.	n.d.	n.d.	n.d.	n.d.	n.d.
0.016	n.d.	n.d.	n.d.	n.d.	n.d.	n.d.
0.004	n.d.	n.d.	n.d.	n.d.	n.d.	n.d.
100.36	100.29	99.32	98.42	97.64	99.74	99.64
H. HARAMURA	T. MIYAKE	T. MIYAKE	Geol. Surv. Japan	G.S.J.	G.S.J.	G.S.J.
1.679–1.683	1.704	1.691	1.685–1.702	1.687–1.700	1.690–1.715 (mean) 1.708	1.688–1.693
56° (avg)	59° (avg)	55° (avg)	51°–56°	30°–50°	56°–48°	54°–52°
none	none	none	none	none	none	titanhematite (100)

basis of 6 oxygens), weights of unit cell and calculated specific gravities

7	8	9	10	11	12	13
1.956	1.790	1.863	1.836	1.918	1.811	1.808
0.029	0.226	0.178	0.350	0.343	0.196	0.195
0.004	0.040	0.019	0.026	0.051	0.064	0.061
0.037	0.089	0.054	0.071	0.052	0.074	0.065
0.016	0.010	0.018	n.d.	n.d.	n.d.	n.d.
0.062	0.138	0.097	0.188	0.334	0.187	0.206
0.002	0.003	n.d.	n.d.	n.d.	n.d.	n.d.
tr.	n.d.	n.d.	n.d.	—	—	—
0.872	0.915	0.938	0.780	0.735	0.803	0.811
1.010	0.770	0.805	0.675	0.401	0.838	0.840
0.008	0.042	0.027	n.d.	n.d.	0.033	0.030
0.003	0.012	0.012	n.d.	n.d.	0.002	0.002
—	—	—	—	—	—	—
6.000	6.000	6.000	6.000	6.000	6.000	6.000
1463.33	1475.36	1457.83	1452.317	1441.29	1485.54	1488.92
3.326	3.364	3.332	3.299	3.283	3.384	3.339

their physical and chemical relations imply the history of crystallization of pyroxenes, details of some examples are presented below.

a. Pyroxenes in pyroxene nodules from Nochi. Clino- and orthopyroxene nodules (websterite) in picrite basalt from Nochi (Fig. 5), in the westernmost part of Okayama Prefecture, were found to have peculiar laminated appearance in a thin section, particularly of clino-pyroxene, and exhibit some abnormal extinction.

The marginal part of the inclusion, which is in contact with the basalt host, has been metamorphosed, separating opaque iron ores and becoming spongy on account of brown glass inclusions in both clino- and ortho-pyroxenes, while the main part of the inclusion remains apparently unaltered.

The orthopyroxene is of Bushveld type with fine exsolution lamellae of diopside.

The clino-pyroxene in question, under microscopic observation, has shown complicated exsolution pattern consisting at least of three phases: diopside-augite-pigeonite which are at first determined by the measurements of optic angles.

The augite lamellae are parallel to (100) of the host. The pigeonite and pigeonitic augite with variable optic angles (2V=0-32°) are banded in the augite lamellae in the direction perpendicular to the plane of augite lamellae, that is

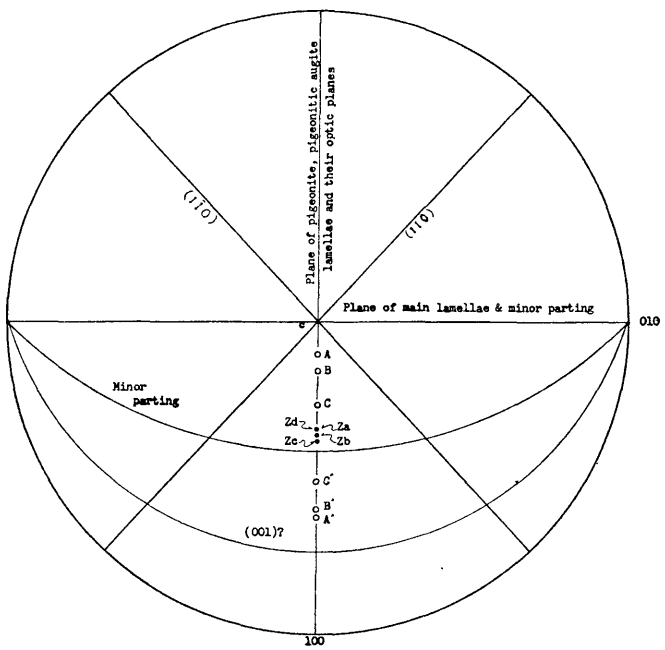

Fig. 10. Optical orientation of exsolution lamellae in aluminian diopsidic augite of websterite inclusion in picrite basalt from Nochi, Okayama Prefecture. A–A′, B–B′, C–C′, and Z_a, Z_b, Z_c, Z_d, indicate the optic axes and optic elasticity axes of each exsolved phases respectively.

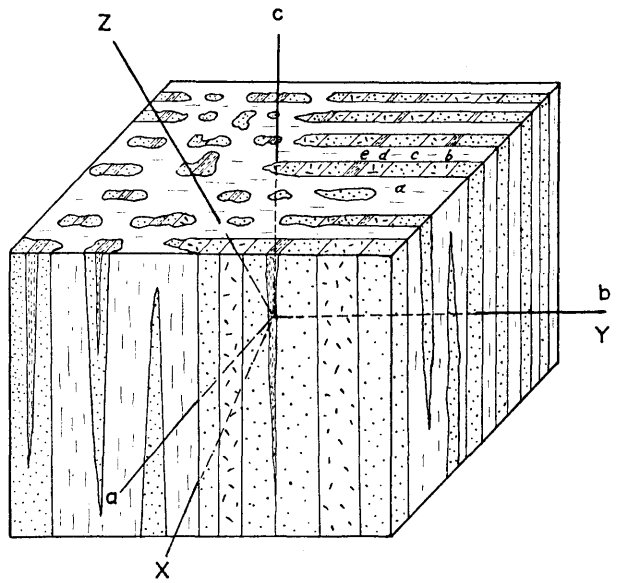

Fig. 11. Aluminian diopsidic augite with broad exsolution lamellae of augite (stipled) parallel to (100) in which are present, in turn, exsolved small lamellae of pigeonitic augite and pigeonite parallel to (010)
optical angle 2V(+)
a=52-54° b=44° c=32° d=24°± e=0°

parallel to (010) of the host pyroxene. The exsolution pattern in thin section is shown in Plate 26, the optical relations of each pyroxene are given stereographically in Fig. 10, and the relations of each pyroxene phase are diagramatically given in Fig. 11.

Under the microscope, however, a very small crystal may be indeterminable, and it is often suspected that the laminated patterns may be due to the twinning and that the variation of optic angles may be also ascribed to the overlapping effect of each lamella as has been often discussed in the case of plagioclase (SUGI, 1940; AOKI, 1959). In this connection, it may be noted that the host pyroxene in question reveals, under high magnification, some moire extinction which is probably due to the very fine lamellar or fibrous crystals arranged parallel to the C-axis of the host pyroxene.

For this reason, to determine the laminated patterns in detail, i.e. to examine whether they are the exsolution product or not, and if possible to obtain the crystallographic relations of these optically variable pyroxene phases, the X-ray analysis by a single crystal oscillation photograph method has been taken. As the exsolved phases are complicated and small in amount, identification by the X-ray powder method was uncertain. The X-ray powder method was used for the determination of the accurate lattice constant of the host pyroxene and for the powdered samples used in the heating experiment.

b. X-ray examination.

(i) Single crystal oscillation photograph—The material used for this study was picked up from one of a pair of sections of pyroxene aggregate (fragment of pyroxene nodule) in picrite basalt used in making thin section. The crystal fragments have three cleavage planes (001), (110) and (110), of which the (001) plane is very perfect. The grain size of 0.15(a)×0.33(b)×0.31(c), 0.10×0.42×0.51, 0.10×0.15×0.38 millimetres, etc. are mounted on glass fibres. More than 30 photographs oscillated about a, b, and c axes of several pyroxenes were taken with a cylindrical camera (camera radius=35.07 mm) with Mn filtered Fe radiation. The spots are very much complicated and cannot be indexed for one pyroxene phase. With the aid of microscopic examination, the indexing was made by trial and error method and a satisfactory result was obtained by assuming that the spots are composed of three phases of pyroxene, diopside, augite and pigeonite.

Some spots split into two and sometimes diffuse. This may be interpreted, coupled with the microscopic examination, that the host pyroxene is composed of slightly twisted aggregate of fine crystals.

The lattice constants obtained by this method are given in Table 9.

Table 9. Cell dimensions of aluminian diopsidic augite with exsolution lamellae of diopside and pigeonite: material from websterite inclusion from Nochi, in the westernmost part of Okayama Prefecture (Measured in the single crystal oscillation photograph)

	Main part (diopside ?)	Exsolved phase (main part of mixture)
a	9.70 Å	9.73 Å
b	8.85 Å	8.94 Å
c	5.23 Å	5.23 Å
β	73°30′	74°30′

(ii) X-ray powder method—Samples of the pyroxene are measured by the X-ray powder method to obtain accurate cell dimensions. Experimental condition is the same as given on page 195. The cell dimensions of the host pyroxene are given in Table 10. Exsolved phases cannot be detected as they present in minor amount.

c. Heating experiment

The margin of the pyroxene nodule is spongy, separating iron ores as mentioned before, having been caused by the pyrometamorphism of the basalt magma. The lamellar structure observed in the central part of the nodule has been disappeared in this margin. In ordr to obtain more information about the thermal history of pyroxene in this nodule, the pyroxene with lamellar structure has been treated by the heating experiments.

Both marginal and central parts of the clinopyroxene have been separated

with the Frantz isodynamic separator. The marginal spongy part of pyroxene contains fine iron ore grains, while the central part of pyroxene is almost free from them. Thus the two part can be readily separated.

The pyroxene with lamellar structure was heated by steps several times in the air in the range of 1160°-1360°C for about 1-10 hours. The mineral was melt partially at about 1210°C and completely at 1350°C.

Upon heating, some oxidized lamellae (pigeonite) were separated with the Frantz isodynamic separator, the remaining unoxidized mineral was treated for repeated heating. On this repeated heating the mineral grains become to show undulate extinction or gradual zoning in which the lamellar structure disappear and approach to homogeneity at about 1170°C for 10 hours heating. The mineral become spongy at 1210°C 1 hour heating separating iron ore grains, which resembles to the natural spongy pyroxene found at the margin of the nodule.

Samples which were heated by several steps and also the unheated and natural spongy samples were measured with the X-ray diffractometer. As a result, selected examples are given in the chart (Fig. 12) and the cell dimensions are also given in Table 10.

The similarity of the heated samples, which become spongy to the natural spongy pyroxene in both optical and structural properties are noted. By continuous heating of the pyroxene, the exsolved phases tend to be homogenized toward one pyroxene phase.

To avoid oxidation, the clinopyroxene with lamellar structure was heated in vacuum (10^{-5} Torr) at 1000°C for about 6 hours. No perceptible change has been recognized about optical and X-ray properties in these experimental condition. Higher temperature and longer time may be necessary for the phase changes.

d. Chemical composition

Chemical compositions of clino- and orthopyroxenes have already been given in Tables 4 and 7.

High alumina content is noted. The minerals may be classified as aluminian diopsidic augite and aluminian bronzite.

e. Remarks

Clino- and ortho-proxenes in pyroxene nodule in basalt from Nochi have exsolution lamellae, in which those of clinopyroxene are very much complicated. Optical and X-ray examinations together with chemical analysis have shown that the clinopyroxene is aluminian diopsidic augite which is exsolved into three phases, diopside, augite and pigeonite. The relation of these phases are shown in Figs. 10 and 11. Optical and structural similarity between the natural spongy rim of pyroxene and the spongy pyroxene obtained by the heating experiment indicates that the former is regarded to have been produced simply by heating effect of the magma and that the condition of this metamorphism (pyrometamorphism) is probably the same as the laboratory experiment. For this reason, the inner part of pyroxene with complicated exsolution pattern must have been free from the effect of the magma. This may indicates that the exsolution

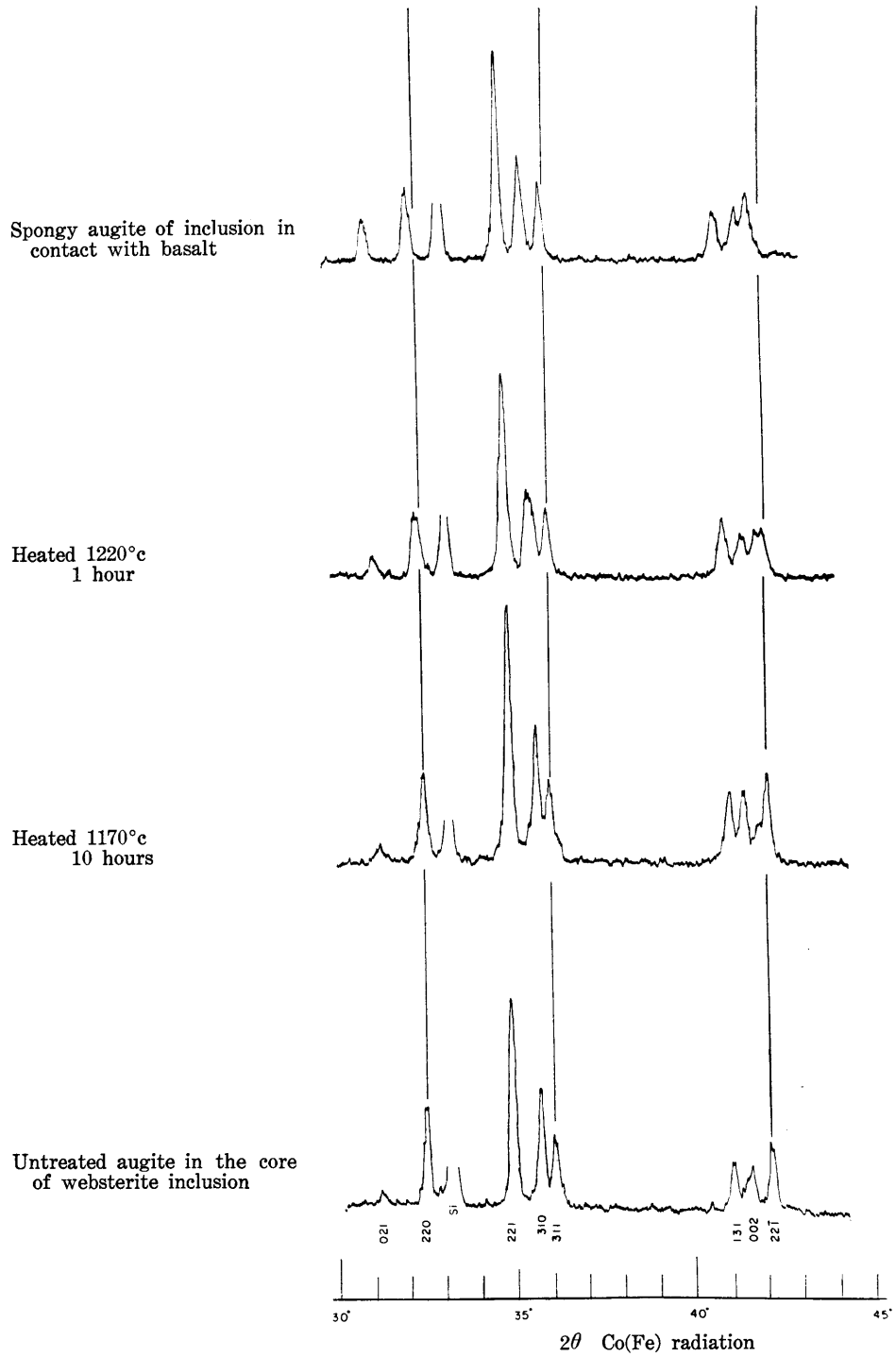

Fig. 12. X-ray powder spectrograms of aluminian diopsidic augites, artificially and naturally heated (spongy rim), in websterite inclusion from Nochi, Okayama Prefecture

lamellae are not ascribed to the pyrometamorphism of the magma but were formed in the course of initial crystallization of the nodule.

The high content of Al and other trivalent cations and the smaller cell volume indicate the condition of crystallization of high pressure and temperature which is to be discussed in chapter IV.

Slow cooling and high pressure (with stress) would probably be the favourable condition for the formation of the very complicated exsolution patterns. The order of the exsolution may be shown as follows.

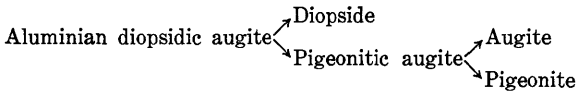

5. *Variation in Cell Dimensions of Clinopyroxenes*

Fine powder of each pyroxene samples separated from various inclusions in basaltic rocks and from phenocrysts in basalts was mixed with powdered silicon as an internal standard and measured with Shimadzu X-ray diffractometer. Peaks for 2θ in the range of angles from 96° to 19° were measured several times in the general survey under the following experimental conditions: copper radiation with a nickel filter at 35 kV and 15 mA, scanning speed 1/2° per minute,

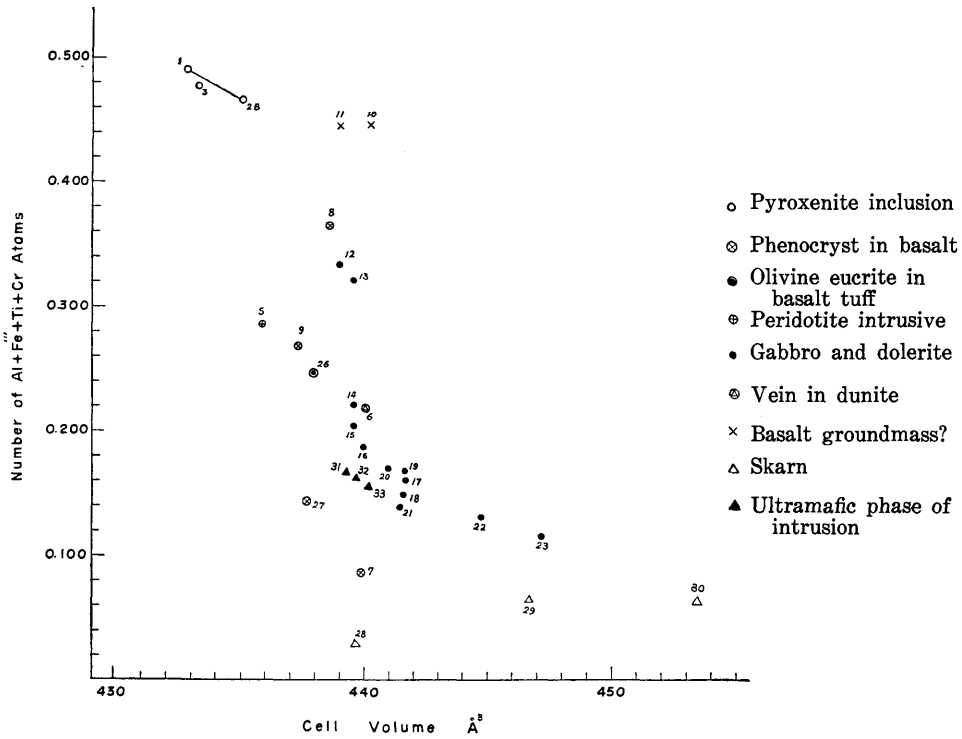

Fig. 13. Variation in cell volume with the contents of Al and other trivalent cations of calcium rich clinopyroxenes. Numbers are refered to Table 10 (data obtained from chemical and X-ray analyses).

Table 10. Cell dimensions, ionic volumes in the cell, packing indices and major cation contents of calcium rich clinopyroxenes. Numbers are refered to pages 185-187.

Sample No.	1	2-B	3	4	5	6	7	8	9	10	11
a sin β (Å)	9.315	9.364	9.289	9.360	9.336	9.360	9.364	9.335	9.344	9.357	9.324
a	9.717	9.769	9.701	9.745	9.720	9.734	9.748	9.728	9.733	9.746	9.736
b	8.849	8.894	8.845	8.890	8.891	8.915	8.918	8.884	8.897	8.896	8.889
c	5.251	5.223	5.274	5.233	5.252	5.274	5.268	5.289	5.262	5.288	5.297
c sin β	5.034	5.007	5.050	5.026	5.045	5.071	5.061	5.075	5.052	5.077	5.073
β	73°28′	73°27′	73°14′	73°50′	73°51′	74°04′	73°52′	73°39′	73°45′	73°46′	73°16′
Unit cell volume (Å^3)	432.85	435.04	433.32	435.42	435.95	440.08	439.92	438.63	437.45	440.17	439.02
Ionic volume (Å^3)	297.05	294.28	296.17	n.d.	297.71	298.37*	299.59	297.90	297.79	295.10	291.64
Packing index	6.863	6.764	6.835		6.830	6.780*	6.810	6.792	6.807	6.704	6.643
Atomic ratio											
Ca	42.8	45.3	39.2	n.d.	45.0	53.6*	51.9	42.2	43.8	41.1	27.3
Mg	46.7	45.3	51.1		52.6	46.0*	44.9	50.2	51.0	47.5	50.0
Fe	10.5	9.4	9.7		2.4	0.4*	3.2	7.6	5.2	11.4	22.7
Number of cations											
Si^{4+}	1.759	1.903	1.775	n.d.	1.833	1.930*	1.956	1.790	1.863	1.836	1.918
Al^{3+} (IV)	0.241	0.097	0.225		0.167	0.030*	0.029	0.226	0.143	0.127	0.000
Al^{3+} (VI)	0.116	0.260	0.155		0.039	0.128*	0.000	0.000	0.035	0.223	0.343
Fe^{3+}	0.103	0.079	0.075		0.025	0.031*	0.027	0.089	0.054	0.071	0.052
Ti^{4+}	0.031	0.029	0.023		0.013	n.d.	0.004	0.040	0.019	0.026	0.051
Cr^{3+}	n.d.	n.d.	n.d.		0.042	0.030*	0.011	0.010	0.018	n.d.	n.d.
2-Si^{4+}	0.241	0.097	0.225	n.d.	0.167	0.070*	0.044	0.210	0.137	0.164	0.082

* doubtful accuracy

Table 10. (continued)

Sample No.	12	13	14	15	16	17	18	19	20	21	22
a sin β (Å)	9.370	9.367	9.363	9.371	9.373	9.375	9.376	9.378	9.383	9.385	9.395
a	9.754	9.747	9.746	9.751	9.753	9.754	9.751	9.753	9.757	9.758	9.763
b	8.905	8.913	8.910	8.926	8.928	8.940	8.945	8.944	8.948	8.954	8.965
c	5.261	5.266	5.268	5.260	5.259	5.270	5.267	5.267	5.251	5.255	5.272
c sin β	5.054	5.061	5.061	5.055	5.054	5.065	5.064	5.064	5.050	5.054	5.073
β	73°52′	73°57′	73°53′	73°57′	73°56′	73°59′	74°06′	74°03′	74°06′	74°07′	74°13′
Unit cell volume (Å^3)	438.98	439.65	439.6	439.6	440.0	441.7	441.6	441.7	441.0	441.5	444.8
Ionic volume (Å^3)	298.27	298.37	297.88	297.40	297.20	296.78	296.76	296.78	296.95	297.27	298.04
Packing index	6.794	6.787	6.776	6.765	6.754	6.719	6.720	6.719	6.733	6.733	6.700
Atomic ratio											
Ca	45.8	45.2	43.4	44.3	44.6	42.3	41.6	40.5	40.9	41.0	40.2
Mg	43.9	43.7	49.1	43.2	40.3	38.7	37.0	36.5	34.5	31.4	27.6
Fe	10.3	11.1	7.5	12.5	15.1	19.0	21.4	23.0	24.6	27.6	32.2
Number of cations											
Si^{4+}	1.811	1.808	1.882	1.904	1.908	1.932	1.937	1.925	1.923	1.924	1.931
Al^{3+} (IV)	0.193	0.195	0.099	0.099	0.091	0.084	0.077	0.086	0.091	0.058	0.063
Al^{3+} (VI)	0.003	0.000	0.040	0.032	0.015	0.018	0.011	0.019	0.010	0.000	0.000
Fe^{3+}	0.074	0.065	0.042	0.047	0.054	0.036	0.036	0.046	0.048	0.044	0.044
Ti^{4+}	0.064	0.061	0.027	0.022	0.025	0.023	0.025	0.018	0.021	0.037	0.024
Cr^{3+}	n.d.	n.d.	0.013	0.004	0.002	n.d.	n.d.	n.d.	n.d.	n.d.	n.d.
2–Si^{4+}	0.189	0.192	0.118	0.096	0.092	0.068	0.063	0.075	0.077	0.076	0.069

Table 10. (continued)

Sample No.	23	24	25	26	27	28	29	30	31	32	33
a sin β (Å)	9.457*	9.486	9.350	9.361	9.341	9.380	9.460	9.547	9.373	9.381	9.382
a	9.802*	n.d.	9.734	9.742	9.744	9.750	9.804	9.854	9.749	9.755	9.756
b	9.004	9.024	8.907	8.901	8.909	8.930	8.980	9.024	8.926	8.932	8.935
c	5.252	n.d.	5.246	5.268	5.260	5.249	5.259	5.263	5.251	5.248	5.252
c sin β	5.067*	n.d.	5.039	5.062	5.043	5.050	5.074	5.099	5.048	5.047	5.050
β	74°45′*	n.d.	73°51′	73°55′	73°28′	74°10′	74°46′	75°40′	74°02′	74°05′	74°04′
Unit cell volume (Å^3)	447.2*	n.d.	436.9	438.9	437.7	439.7	446.7	453.4	439.3	439.7	440.2
Ionic volume (Å^3)	299.70	300.21	n.d.	298.62	297.88	299.01	300.23	301.04	297.40	297.06	297.11
Packing index	6.705*	n.d.	n.d.	6.804	6.806	6.800 (6.751)	6.721 (6.553)	6.640 (6.526)	6.770	6.756	6.749
Atomic ratio											
Ca	42.8	44.5	44.3	47.2	41.4	49.2	50.5	52.4	42.3	39.5	37.6
Mg	11.1	2.0	49.6	43.2	47.8	47.2	17.5	3.6	46.0	42.5	41.1
Fe	46.1	53.5	6.1	9.6	10.8	3.6	32.0	44.0	11.7	18.0	21.3
Number of cations											
Si^{4+}	1.941	1.928	—	1.851	1.911	1.986	1.991	1.988	1.933	1.936	1.927
Al^{3+} (IV)	0.051	0.068	0.094	0.149	0.089	0.012	0.027	0.015	0.067	0.064	0.073
Al^{3+} (VI)	0.000	0.038	0.051	0.065	0.005	0.005	0.022	0.000	0.051	0.039	0.035
Fe^{3+}	0.044	0.052	—	0.022	0.027	0.011	0.014	0.047	0.037	0.045	0.036
Ti^{4+}	0.021	0.002	—	0.011	0.022	0.001	0.002	0.002	0.012	0.015	0.011
Cr^{3+}	n.d.	n.d.	—	n.d.	n.d.	n.d.	n.d.	n.d.	0.000	0.000	0.000
2-Si^{4+}	0.059	0.072	—	0.149	0.089	0.014	0.009	0.012	0.067	0.064	0.073

* doutful accuracy

Table 10. (continued)

Sample No.	34	35	36	37	38	39	40	41	42	43	44	45	46
Specific gravity (observed)	3.332	3.329	3.322	3.323	3.312	3.311	3.311	3.320	3.305	3.303	3.271	3.32(?)	3.315
Unit cell volume (Å^3) (calculated)	432.19	435.31	435.92	436.03	437.43	435.92	438.59	440.52	443.94	439.61	443.10	435.79	462.65
Ionic volume (Å^3)	295.95	297.66	297.52	297.24	298.11	296.79	298.01	297.77	297.47	298.78	298.57	298.28	315.30
Packing index	6.848	6.838	6.825	6.817	6.815	6.808	6.795	6.759	6.700	6.796	6.738	6.845	6.815
Atomic ratio													
Ca	43	45	46	43	44	40	47	43	43	47	46	49	46
Mg	53	51	50	52	52	55	49	51	50	49	50	49	38
Fe	4	4	4	5	4	5	4	6	7	4	4	2	16
Number of cations													
Si^{4+}	1.920	1.864	1.882	1.831	1.899	1.847	1.878	1.904	1.838	1.964	1.958	1.971	1.982
Al^{3+}	0.153	0.255	0.220	0.282	0.175	0.275	0.202	0.075	0.197	0.031	0.029	0.054	0.200
Fe^{3+}	0.031	0.039	0.048	0.042	0.022	0.023	0.019	0.045	0.069	0.000	0.004	0.060	0.058
Ti^{4+}	0.017	0.006	0.011	0.022	0.022	0.007	0.009	0.018	0.020	0.004	0.004	0.001	0.020
Cr^{3+}	0.062	0.023	0.028	0.027	0.042	0.034	0.030	0.028	0.035	0.020	0.025	0.008	n.d.
$2\text{-}Si^{4+}$	0.080	0.136	0.118	0.169	0.101	0.153	0.122	0.096	0.162	0.036	0.042	0.029	0.018

Table 10. (continued)

Sample No.	47	48	49	50	51	52	53	54	55	56	57	58	59
Specific gravity (observed)	3.299	3.383	3.445	3.373	3.285	3.397	3.394	3.414	3.420	3.358	3.384	3.364	3.385
Unit cell volume (Å^3) (calculated)	440.10	441.90	444.48	446.48	454.21	457.34	442.56	445.61	443.81	442.80	443.26	444.34	443.20
Ionic volume (Å^3)	296.70	297.57	299.28	299.62	298.09	298.42	298.27	298.73	299.48	298.53	298.76	299.33	298.48
Packing index	6.742	6.734	6.733	6.711	6.563	6.525	6.740	6.704	6.748	6.742	6.740	6.737	6.735
Atomic ratio													
Ca	40	41	49	51	46	43	45	46	50	47	46	48	46
Mg	53	42	28	37	36	23	38	31	34	41	39	40	38
Fe	7	17	23	12	18	34	17	23	16	12	15	12	16
Number of cation													
Si^{4+}	1.912	1.904	1.868	1.888	1.911	1.959	1.921	1.937	1.939	1.926	1.915	1.957	1.925
Al^{3+}	0.127	0.117	0.197	0.117	0.211	0.106	0.119	0.124	0.074	0.107	0.106	0.061	0.111
Fe^{3+}	0.031	0.032	0.061	0.086	0.039	0.055	0.053	0.069	0.128	0.057	0.053	0.093	0.058
Ti^{4+}	0.007	0.029	0.021	0.007	0.016	0.008	0.011	0.007	0.008	0.009	0.008	0.005	0.008
Cr^{3+}	0.035	0.005	n.d.	n.d.	n.d.	n.d.	n.d.	n.d.	0.000	0.000	0.000	0.001	0.000
2-Si^{4+}	0.088	0.096	0.132	0.112	0.089	0.041	0.079	0.063	0.061	0.074	0.085	0.043	0.075

Table 10. (concluded)

Sample No.	60	61	62	63	64	65	66	67	68	69	70	71
Specific gravity (observed)	3.382	3.303	3.364	3.332	3.324	3.314	3.377	3.278	3.373	3.342	3.276	3.280
Unit cell volume ($Å^3$) (calculated)	444.39	445.26	444.80	443.80	446.07	437.3	443.1	441.2	447.2	446.4	450.5	453.9
Ionic volume (Å)	298.59	299.15	298.71	297.93	298.77	297.94	298.84	296.92	299.02	298.34	298.16	298.82
Packing index	6.719	6.719	6.715	6.713	6.698	6.812	6.745	6.731	6.687	6.683	6.619	6.579
Atomic ratio												
Ca	46	49	46	47	46	46.5	45.5	40.7	46.0	45.7	42.8	46.6
Mg	40	44	38	43	45	48.0	36.8	52.3	32.1	36.5	44.8	37.8
Fe	14	7	16	10	9	5.5	17.7	7.0	21.9	17.8	12.4	15.6
Number of cations												
Si^{4+}	1.898	1.947	1.917	1.913	1.872	1.891	1.825	1.852	1.770	1.737	1.837	1.813
Al^{3+}	0.106	0.062	0.155	0.115	0.134	0.205	0.245	0.248	0.255	0.344	0.148	0.230
Fe^{3+}	0.096	0.034	0.040	0.048	0.042	0.025	0.112	0.038	0.224	0.158	0.123	0.112
Ti^{4+}	0.016	0.004	0.010	0.008	0.011	0.007	0.040	0.013	0.050	0.059	0.056	0.060
Cr^{3+}	0.000	0.000	0.002	0.001	0.002	0.023	0.000	0.017	0.000	0.000	0.000	0.001
$2\text{-}Si^{4+}$	0.102	0.053	0.083	0.087	0.128	0.109	0.175	0.148	0.230	0.263	0.163	0.187

chart speed 10 millimetre per minute, time constant 5, slit 1-1-0.2 mm. Some selected peaks at higher angles were also measured repeatedly with more slow scanning speed (1/8° per minute). Each reflection plane were indexed and the unit cell dimensions a, b, c and β were determined in the same way as mentioned in my previous paper (YAMAGUCHI, 1961a). The accuracy for the cell dimensions is ± 0.001 Å.

The newly investigated unit cell dimensions, together with the pre-existing data from plutonic and volcanic pyroxenes (BROWN, 1960; KUNO, 1955), are listed in Table 10. The occurrence and short notes of these minerals are already given in section **3** of this chapter.

From these data, the relation between cell volumes and the content of Al and other trivalent cations are graphically given in Fig. 13.

The figure indicates that the cell volume of plutonic clino-pyroxene decreases with the increase of trivalent cations.

6. The Banded Structure (Translation Lamellae) of Olivines

So far as the available samples are concerned, the olivine crystals, constituents of ultrabasic inclusions in basalts and limburgites, are characterized by the presence of translation lamellae and strongly strained nature due to wavy extinction. The characters have been repeatedly stressed in the description of the previous section.

Generally, these olivine crystals are subhedral, clear and free of inclusions. They exhibit several broad banding due to translation, the slip planes are nearly normal to the *a* axis of the crystals. The most strongly banded texture has been found in the peridotite inclusion in limburgites from Ôguso-yama (Plate 25).

The translation lamellae of olivine have already been noted by TURNER (1942) in the peridotitic rocks from New Zealand. He concluded that such banding of olivine in the peridotite is due to the laminar flow in a partially, perhaps almost completely crystallized magma.

I have also recognized such banded structure of olivine in the dunite or peridotite from Akaishi, Shikoku and from Horoman, Hokkaido (YAMAGUCHI, 1961a). The banded olivine occurs in the peridotite or dunite of schistose nature, but is lacking in the massive rocks. The schistose periodtites are often composed of aggregates of coarse grains of olivine in lenticular forms in the fine grained matrix. In these examples, only the coarse olivine grains show translation lamellae. For this reason, shearing stress may probably be the main factor to produce the translation lamellae of olivine crystals.

Olivine in olivine gabbro inclusion from Dôgo exhibit feeble or no translation lamellae.

III. Recrystallization of Serpentinite to Dunite

From the north of Hokkaido to the southwest of Kyushu, ultrabasic rocks occur in many places along the island arcs of Japan. Most of these ultrabasic

rocks are serpentinite which were probably derived from peridotite or pyroxenite. The most conspiceous body of fresh unaltered peridotite or dunite in Japan is found in the migmatite zone of the Hidaka metamorphic complex, Hokkaido (at Horoman and Horoshiri) and in the spotted schist zone of the Sambagawa crystalline schist of Shikoku (at Higashi-Akaishi), some of which are briefly described in my previous paper (YAMAGUCHI, 1961a). Minor bodies of unaltered rocks also occur locally.

SEKI (1951) described the ultrabasic rocks from Miyamori, Iwate Prefecture, which are composed mainly of tremolite serpentinite and diopside-hornblende rocks. These rocks (5~10×20 km) were intruded into the palaeozoic formation and were affected by later granodiorite intrusion. The contact metamorphism of this granodiorite transformed the ultramafic rocks (about 2-4 km in width), resulting in the recrystallization of olivine, tremolite, talc, chlorite, diopside, brown hornblende, green hornblende, ilmenite, sphene, epidote, leucoxine, cummingtonite, spinel, antigorite etc., which are divided into several metamorphic zones from their mineralogical assemblages in the rocks. SEKI (1951) concluded that the interaction between serpentinized periodtite and the intrusive granodiorite is responsible for the formation of these metamorphic zones where the increase of the contents of SiO_2 and MgO and the decrease of the contents of Fe_2O_3+FeO, Na_2O+K_2O, Al_2O_3 and TiO_2 are found as the metamorphic rocks are closer to the contact with the granodiorite. Similar conclusion has also been expressed by REED (1934) on the metamorphic rocks derived from serpentinite which was captured in gneissose rocks.

I have also examined some dunites which were probably derived by recrystallization from serpentinite as are explained in the following section.

1. Serpentinite and Dunite from Obira Mine and Its Environs, Ôita Prefecture

Ultrabasic rocks occurring in parallel with the Usuki-Yatsushiro Line, the southwestern extension of the Median Dislocation Line in Kyushu, generally belong to serpentinite which contains only a trace of olivine and/or pyroxene derived probably from peridotites or pyroxenites. The one exception is a fresh dunite composed essentially of olivine which occurs around Obira Mine, Ôita Prefecture.

Microscopic examination of several samples of the ultramafic rocks collected from this area shows that the dunite is the product of recrystallization from serpentinite developed in this region. Several stage of metamorphism have been recognized as in the following:

Serpentinite
↓
Tremolite-serpentinite
↓
Serpentine-tremolite-olivine rock
↓
Dunite

Some veinlets composed essentially of olivine occur cutting through serpentinite (Fig. 14). Sometimes, olivine occurs as porphyroblastic crystals in the

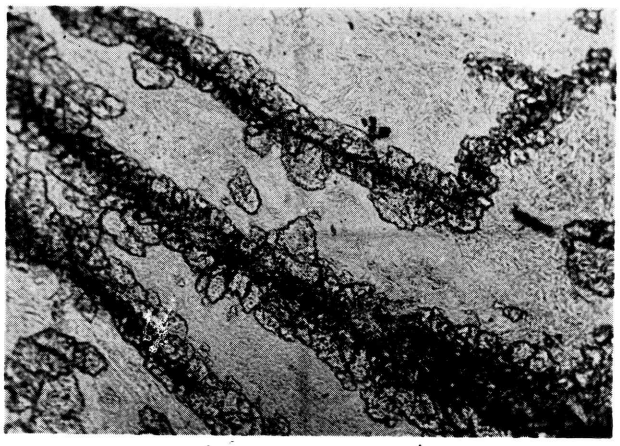

Fig. 14. Olivine vein cutting through serpentinite (open Nicols)

serpentinite (Fig. 15). The recrystallized olivine contains abundant minute inclusions of iron ores. It is considered that the recrystallization is the result of thermal metamorphism affected by the late intrusion (probably of Miocene) of granite and its ring dyke (granite-porphyry) developed in this region.

It is a well known fact that during serpentinization the mafic minerals are generally altered to serpentine giving rise at the same time to minute grains of iron ores. The minute grains of iron ores included in the recrystallized olivine may be regarded as those separated during serpentinization and then enclosed at the time of recrystallization.

2. *Dunite from Higashi-Akaishi, Shikoku*

In some massive dunite from Higashi-Akaishi, Shikoku (YAMAGUCHI, 1961a),

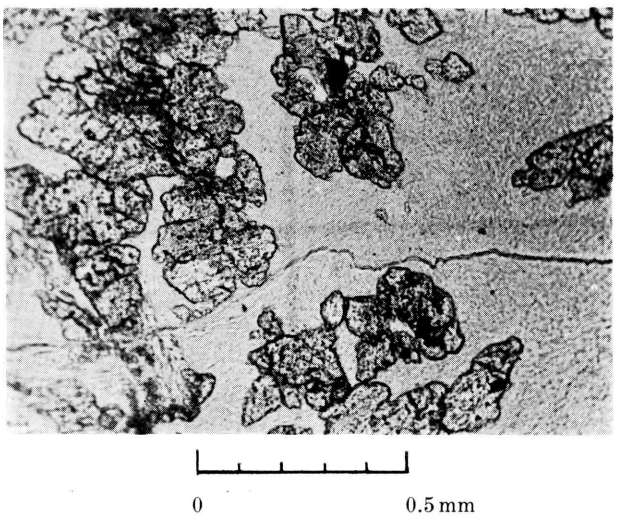

Fig. 15. Porphyroblastic crystal of olivine in serpentinite (open Nicols)

two types of olivine have been recognized: the one is clear and the other is turbid, containing abundant minute inclusions of iron ores.

There is no notable difference in the optical properties between these two kinds of minerals. Translation lamellae have not been detected. However, by the high Ca content the clear olivine is distinguishable from turbid one as is shown in Table 11.

Table 11. Lime contents in clear and turbid olivine crystals of dunite from Higashi-Akaishi, Shikoku, Japan
(Determined by EDTA titration method)

	CaO (wt. per cent.)		
Sample No.	Clear olivine	Slightly turbid olivine	Turbid olivine
AK 29-1e	0.78		
AK 55-3	0.64	0.26 0.32	0.35
AK 53	0.60	0.32	0.25
AK 25-4	n.d.	0.36	n.d.
AK 49-1e	n.d.		0.22

The Higashi-Akaishi dunite occurs in the spoted schist zone, the highest grade of metamorphism among the Sambagawa crystalline schist developed in this region. Ultrabasic rocks distributed in the lower grade metamorphic zone in this region belong in most part to serpentinite. This field relation and also the occurrence of turbid olivine beside the clear olivine indicate that the Higashi-Akaishi dunite has been in some part (if not all) recrystallized from olivine serpentine rocks.

3. Remarks

Recrystallization of serpentinite to dunite by thermal metamorphism is not unusual in the present state of knowledge. The experiment of BOWEN and TUTTLE (1949) is particularly interesting. Their result shows that

brucite + serpentine $\rightleftharpoons$ forsterite + vapour

at about 400°C at the lower pressure and at only slightly higher temperature at the higher pressure, and

Serpentine $\rightleftharpoons$ talc + forsterite + vapour

at 500°C at every pressure. For all practical purposes, pure magnesian serpentine can not exist at temperature above 500°C.

Natural olivine containing 10 per cent. fayalite which found in many ultramafic rocks is serpentinized at 340°C and 15,000 lbs/in^2 (BOWEN and TUTTLE, 1949). The reverse is also expected which means at this lower temperature serpentine transforms to olivine. Serpentinite of California (MACDONALD, 1941, 1942) metamorphosed by the intrusion of quartz diorite stocks also indicates

such trasnformation, where grains of olivine are quite commonly poikiloblastic, enclosing smaller grains of serpentine, talc and iron ores.

If the serpentinite in the crust were captured in basaltic magma on their way to the surface, recrystallization or pyrometamorphism of serpentine to olivine could possibly occur. However, recrystallized olivine is generally of turbid crystals containing many fine grains of iron ores and other minerals, as indicated in the dunites from Obira and Higashi-Akaishi and others. So far as my observation goes, such minerals could not been found in the investigated ultrabasic inclusions. Dunitic rocks included in the basalt of Southwest Japan are for this reason interpreted to have been derived from another source.

IV. Packing Index of Clinopyroxene

The conception of packing index has been proposed by FAIRBAIRN (1943) to give quantitative values to the ratio ion volume/unit cell volume of minerals. According to FAIRBARN, the role of packing index in thermal inversion and incongruent melting is believed to be accessory for the most part, but in pressure inversion it plays a vital role. It is also an important factor in controlling the maximum size of the minor ions which may enter a crystal structure.

The packing indices given by FAIRBAIRN (1943) were of approximate value for many kinds of minerals, however, the general tendency of his calculation was sufficient enough to consider that minerals formed at higher pressure as estimated from many kinds of geological evidence give higher packing indices.

Through my study of the cell dimensions of clinopyroxenes in ultrabasic inclusions, a smaller cell volume than the usual clinopyroxene has been noted. Since this material is assumed to have come from the depth, the higher packing index can be expected. For this reason, accurate determination of the packing index was attempted to obtain the difference among the clinopyroxene species crystallizd at different conditions, though the values given by FAIRBAIRN (1943) were in the range of 5.9 to 6.0.

1. Procedure

The closeness of ion packing in a crystal can be calculated according to the following formula.

$$V_{abs}=\frac{V_{cell}}{Z}=\frac{W_{mol}}{N.D}=\text{Vol. ions}+\text{Vol. ``interstices''}$$

$$\text{Packing Index P.I.}=\frac{V_{ions}}{V_{cell}}\times 10$$

The calculations are also based on the following quantities

$$W_{abs}\ \text{(in grams)}=\frac{W_{cell}}{Z}=\frac{W_{mol}}{N}$$

where

V_{abs}=absolute volume
V_{cell}=volume of unit cell
V_{ions}=volume of ions
W_{mol}=molecular weight
W_{abs}=absolute weight

W_{cell}=weight of unit cell
D=density
Z=the number of formula units in the cell
N=Avogadro's number

Clinopyroxene is obviously of ionic minerals, the volume of ions was calculated from the standard formula of clinopyroxene which was calculated from the chemical analysis. The ionic radii used were referred to the work of PAULING (1960) which are reproduced in Table 12. The atomic weight was taken from the International Atomic Weight Tables (1960), the AVOGADRO's number used was $N=6.02486\times10^{23}$, and the number of formula units in the cell of clinopyroxene is Z=4.

The volume of unit cell has been calculated in two ways, the one is calculated from the determination of accurate cell dimensions by the X-ray powder method described in the previous section of this paper, the other is calculated from chemical compositions and specific gravities listed in the up-to-date literature.

The material used was confined to the calcium rich clinopyroxene with a definite crystal structure. Calcium poor clinopyroxene was omitted as its structure is slightly different.

2. *Result and Discussion*

Packing indices calculated in two ways as mentioned above are listed in Table 10 together with other major variable quantities. Of several samples, of which the cell dimensions and the specific gravities were determined, the packing indices calculated on both quantities are not in accordance with each other. The discrepancy of this calculation is due mainly to the inaccuracy in the determination of specific gravity.

The relations of packing index to other variable cation contents in clinopyroxene were examined in various ways, in which the relation of the contents

Table 12. Ionic radius, calculated and empirical value after PAULING (1960), used for the calculation of packing index (Ionic volume calculated by the writer)

Element	Radius (Å)	Volume (Å^3)
P^{5+}	0.34	0.1646
Si^{4+}	0.41	0.2887
Al^{3+}	0.50	0.5236
V^{5+}	0.59	0.8603
Fe^{3+}	0.64	1.0981
Mg^{2+}	0.65	1.1503
Ti^{4+}	0.68	1.3171
Cr^{3+}	0.69	1.3761
Ni^{2+}	0.72	1.5635
Co^{2+}	0.74	1.6974
V^{3+}	0.74	1.6974
Fe^{2+}	0.76	1.8388
Mn^{2+}	0.80	2.1447
Na^{1+}	0.95	3.5914
Ca^{2+}	0.99	4.0644
K^{1+}	1.33	9.8547
O^{2-}	1.40	11.4940
(OH^{1-})	(1.40)	(11.4940)

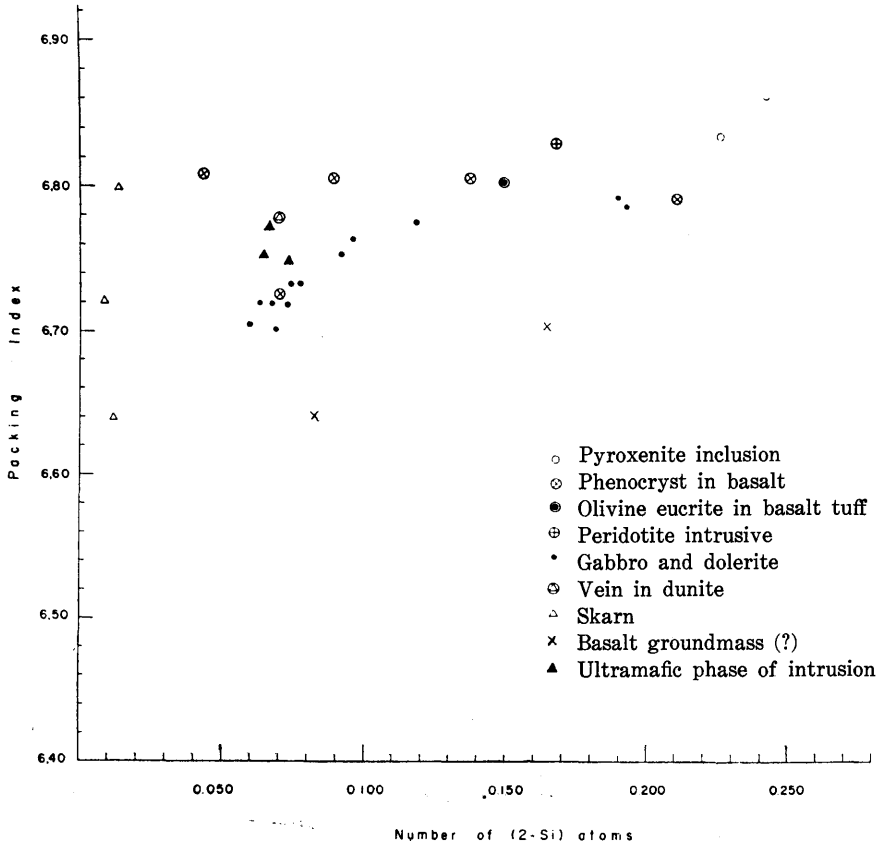

Fig. 16. Relationships between packing index and number of (2–Si) atoms for calcium rich clinopyroxenes (data obtained from chemical and X-ray analyses)

of Si atoms to the packing index was satisfactory for understanding the geological relationships of these variable clinopyroxenes. The relations are graphically shown in Figs. 16 and 17. It is noted that the minerals of ultrabasic inclusion in basaltic rocks are remarkably high both in the packing index and the contents of (2−Si) atoms. Among the samples of ultrabasic intrusive rocks, some are the same as that of the inclusion (i.e., Horoman peridotite) others are nearly equal in packing index but lower in the number of (2−Si) atoms.

The linear relation of clinopyroxene in the Skaergaard rocks is particularly worthy of notice. As the crystallization proceeds, i.e. with falling temperature and probably pressure, the packing index and the number of (2−Si) atoms decrease. Other rocks, such as gabbro, diorite, granite and syenite also show approximately the same general tendency to that of the Skaergaard with falling temperature and pressure as estimated from their geological occurrences.

There are some exceptions. Clinopyroxene in the gabbro inclusion from Hawaii is high in (2−Si), but similar in packing index to the Skaergaard rocks. Some pyroxenite and gabbro xenolith in monchiquite from New South Wales

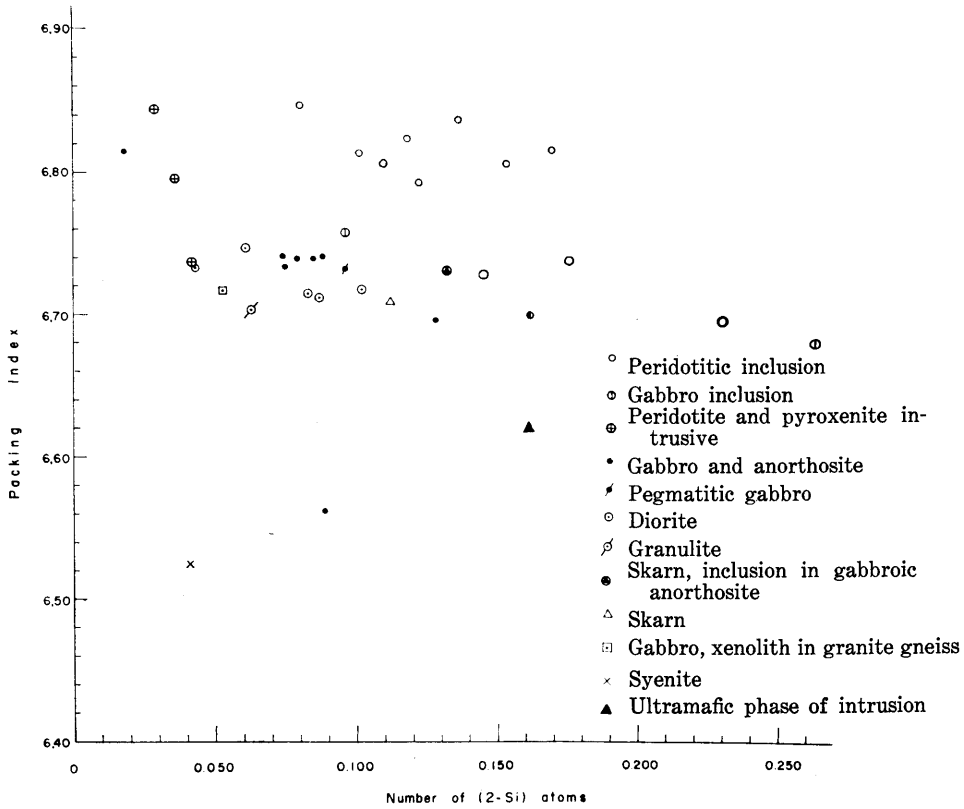

Fig. 17. Relationships between packing index and number of (2-Si) atoms for calcium rich clinopyroxenes (data obtained from chemical compositions and specific gravities)

(WILSHIRE and BINNS, 1960) are high in (2—Si) in their clinopyroxene but lower in packing index, being somewhat dissimilar to other inclusions in basaltic rocks. It is not clear at present whether these differences are due to the less accuracy in the calculation of cell volume by the specific gravities than in that by X-ray determination or otherwise. These inclusions would probably represent certain source rocks which are different from those of other inclusions in basaltic rocks.

Generally, the change of packing index during crystallization is governed by two important variables, i.e. the arrangement of the dominant tetrahedra in the crystal structure and the size of the cations linking the fundamental tetrahedra with each other. Aluminum with the coordination numbers of 4 and 6, tends to enter both in tetrahedral and octahedral positions. High temperature and low pressure favour low coordination, and low temperature and high pressure favor high coordination (MASON, 1952). Higher the coordination is, more economical the space is. Thus at higher temperature, aluminum tends to enter into the tetrahedral position replacing Si ions in the pyroxene, whereas at lower temperature it tends to enter into the octahedral position. Since a mineral requires its electrical stability in the structure, substitution of Al ions for Si

ions naturally introduces other trivalent cations into the octahedral position so as to balance the charges. An example of substitution has been described previously (YAMAGUCHI, 1961a). If the contents of Al ions were sufficient during certain conditions of pyroxene crystallizatoin, sharing of Al ions in both tetrahedral and octahedral positions could occur according to the temperature and pressure relations. Combined effect of this substitution tend to decrease the cell volume, and hence the increase of packing index of pyroxenes.

The cell volume varies in clinopyroxene in relation to the ratios of major Ca:Mg:Fe ions. Packing index is however, an independent variable, the effect of atomic weight variable being eliminated and evidently indicates the closeness of ion packing. The ion packing naturally implies the important relation to pressure or stress in the formation of minerals as has also been indicated by FAIRBAIRN (1943). Accordingly, the crystal-chemical behavior of cations in the structure and the described geological evidence indicate the possibility that the packing index of calcium rich clinopyroxene may be used as a key of geological barometer. The number of Si ions, or the number of cations entering the tetrahedral position may be of vital problem, although there is an indication that the number of (2−Si) atoms may also be used as the temperature indicator.

V. The Petrogenic Significance of Ultrabasic Inclusion in Basaltic Rocks from Southwest Japan

1. Origin of Ultrabasic Inclusion and their Relation to Ultrabasic Intrusive Rocks

Derivation of ultrabasic rocks by crystal settling of early formed minerals in basaltic magma has often been considered (BOWEN, 1928; HARUMOTO, 1951; and many others). However, the Mg/Fe ratios of olivine and pyroxene in ultrabasic inclusion are significantly higher than those in the corresponding minerals crystallized from basaltic rocks. Most olivines in peridotitic intrusive rocks and of peridotitic inclusions in basalt have the composition of about Fa10, while those from basalts are nearly of Fa20 (this paper, ÔJI, 1961a, 1961b). The presence of chromian diopside and spinel in ultrabasic rocks is also of significant meaning as compared with the constituents of basaltic rocks. Further, most ultrabasic inclusions are the angular rock fragments torn up into pieces of consolidated rocks, and the constituent minerals are often mosaic and strongly strained. They are often decomposed at the contact of the basalt host by the heat effect of magma, which reconstructed their composition so as to approach to that of basalt phenocryst. These evidences would preclude the origin of ultrabasic inclusion by differentiation of the basalt itself.

In their detailed studies of olivine rich inclusions in basaltic rocks, ROSS, FOSTER and MYERS (1954) have shown a very close similarity in mineralogical and chemical relationships of these inclusions to dunitic and peridotitic intrusive rocks. They considered, as in the current way, that the ultramafic intrusive rocks have come to their place by 'solid intrusion' from the peridotite mantle of the

earth after the profound orogenic movements. On the other hand, it has been generally considered that the ultrabasic inclusions represent either unchanged mantle material captured by the basalt magma in their way to the surface or the less fusible portion of the mantle material from which the basalt was formed by partial remelting. Seismological observation of the volcanic activity in Hawaii for example, shows that the basalt magma appears to have come from the depth, well below the Mohorovičič discontinuity (POWERS, 1955; MACDONALD, 1961), and its ultrabasic inclusions can reasonably be expected to have come from the same region. For this reason, the nature below the Mohorovičič discontinuity has been our special concern. LOVERING (1958) suggested that a layer of eclogite with the chemical composition of basalt extends to a depth of 100 km. in the earth and that the Mohorovičič discontinuity represents the phase transformation from basalt to eclogite. KUNO (1959) has raised argument against LOVERING's hypothesis, emphasizing the significance of ultrabasic nodules, and has pointed out that eclogitic and gabbroic inclusions are not associated in basaltic rocks, although this would be expected if the gabbro layer were directly underlain by an eclogite layer of gabbroic composition. LOVERING (1959) mentioned in reply an association of eclogite, pyroxene-granulite, and peridotite inclusions in alkali-basalts of eastern Australia. He, furthermore, mentioned the predominance of granulitic and eclogitic inclusions over peridotitic inclusion. Hypersthene eclogite in basalt tuff from Hawaii has also been described recently (YODER and TILEY, 1962). However, the recorded occurrence of inclusions in the world seems to indicate that the peridotitic inclusions still predominate over the eclogitic ones. suggesting the greater importance of peridotitic rocks than eclogite in the region of basaltic formation (refer ROSS and others, 1954).

Inclusions in basaltic and limburgitic rocks from Southwest Japan are of dunitic, peridotitic, pyroxenitic and gabbroic rocks. No eclogitic rocks have been found. Garnet bearing rocks such as garnet amphibolite or eclogite are seldom found in the Sangun metamorphic zone or in the Sambagawa crystalline schist system. The rather typical eclogitic rocks are found in the layered ultrabasci body at Higashi-Akaishi, Shikoku as already mentioned. Eclogite at this place occurs in the forms of small lenticular mass within dunite or pyroxenite with sharp boundaries from the adjoining rocks. Layered or banded structure composed of monomineralic rocks of dunite and pyroxenite, and the presence of eclogite in this ultrabasic intrusive rocks may probably be ascribed in part to a high grade of metamorphism and tectonic movements. However, basaltic rocks found around this region do not contain any eclogitic inclusion.

The petrographic and mineralogical similarity of ultrabasic inclusions in basaltic rocks to those of ultrabasic intrusive rocks is worthy of notice. The constituents of ultrabasic inclusions are, however, more strongly strained that those of common ultrabasic intrusive rocks. The exsolution pattern in pyroxenes of inclusions is very much complicated. The mineral contains a remarkably high amount of Al ions replacing Si ions in the structure. Their smaller cell volumes and the higher packing indices than in other igneous rocks are also noticeable

(Table 10, Figs. 13, 16, 17). This evidence indicates that most ultrabasic inclusions should be distinguished from ultrabasic intrusive rocks. The ultrabasic incusion in question should be derived from more profound depth of higher pressure and temperature than many accessible ultrabasic intrusive rocks.

Some gabbroic inclusions may have had a slightly different history. According to ROSS and others (1954), gabbroic nodules of the 1801 Kaupulehu flow of Hualalai, Island of Hawaii, composed of calcic plagioclase and olivine or diopside, do not present a feature of direct crystallization from a basalt magma. They explained these rocks to have been derived from a zone in the earth's crust somewhat higher than that of the olivine-rich nodules. In the present study, the relation of (2−Si) ions to the packing indices shows that these olivine gabbro inclusions are closely related to the intrusive gabbroic rocks such as those of Skaergaard. Olivine gabbro inclusions such as found in the basalt from Dôgo and others may have been derived from such intrusive gabbroic rocks.

2. *Ultrabasic Inclusions in Relation to Basaltic Rocks*

Many ultrabasic inclusions are generally found in the alkali-olivine basaltic rocks, while they are rare in tholeiitic basaltic rocks. This is quite an important fact for the solution of basalt petrogenesis, in view of the hypothesis that the tholeiitic magmas are also considered as come from below the Mohorovičič discontinuity. Complete remelting of eclogitic rocks below the Mohorovičič discontinuity as in the model of LOVERING (1958) and YODER and TILLEY (1962) may be one of the explanations for tholeiite production. Some basaltic rocks containing fairly large amount of alumina (KUNO, 1960) which are believed to have come from greater depth include a few ultrabasic rocks. However, the source of high alumina is still questionable and is often considered as the result of contamination of sialic materials (TOMITA, 1958). In this connection, the effect of basaltic magma to the ultrabasic inclusions should be noted. Constituent minerals of ultrabasic inclusions have often been decomposed at the margin; olivine has changed to finer crystals with Fa richer composition, orthopyroxene

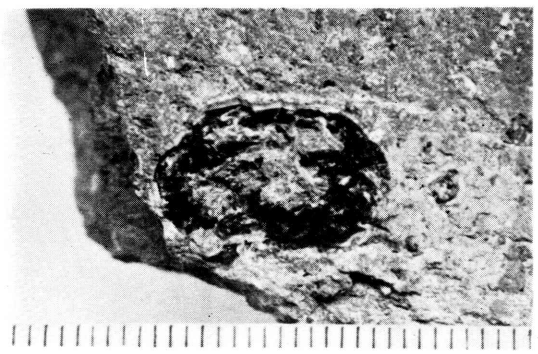

Fig. 18. Megascopic feature of pseudo-hypersthene, xenocryst separated from ultrabasic inclusion in olivine basalt from Shimo-ganya. Note the crustal layer (grey) composed of olivine and pigeonite aggregates.

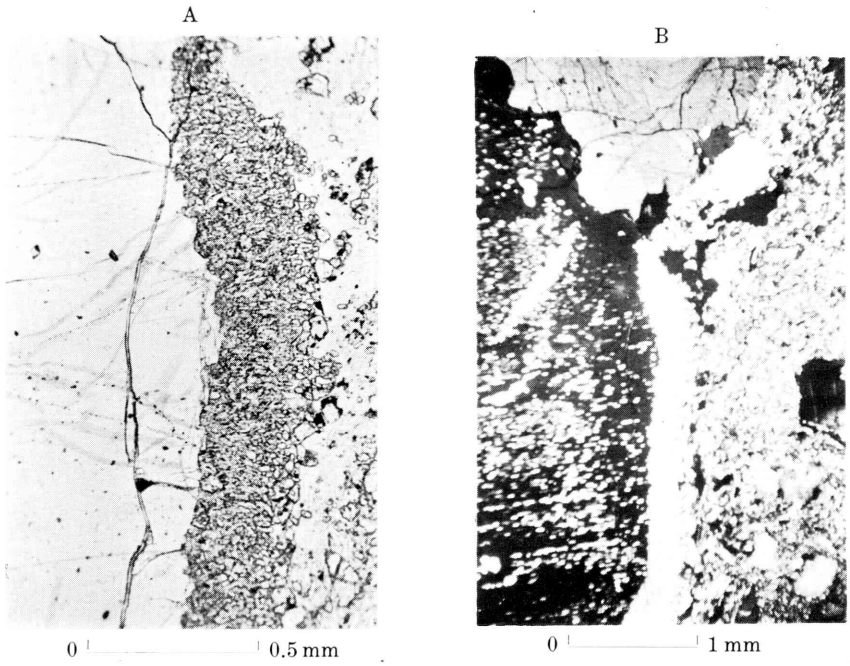

Fig. 19. A) Marginal part of bronzitite inclusion showing the formation of pseudohypersthene, composed of bronzite and surrounding outer zone of olivine and pigeonite aggregates, along the boundary in contact with the host basalt (parallel Nicols). B) Same part as A). Note the exsolution lamellae of diopside (white) in bronzite. Phenocryst in the right is olivine showing wavy exrinction (crossed Nicols).

has reconstructed to aggregate of olivine and pigeonite (Figs. 18 and 19) (pseudohypersthene of TOMITA, 1936), clinopyroxene is spongy separating glass and iron ores, and thus the remaining pyroxene often becomes somewhat diopsidic in composition (Table 7, No. 28). Such reconstructed minerals derived from ultrabasic inclusions are often disintegrated mechanically and found as isolated xenocrysts. If the ultrabasic inclusions were not recognized in the basaltic rocks, such xenocrysts could ont be recognized as derived from the inclusions and would be easily misidentified as phenocrysts crystallized from basalt magma.

An example may be a large phenocryst of augite in basalt from Nishigatake, Saga Prefecture. Black type augite (Table 7, No. 8) in the core of green type augite (Table 7, No. 9), containing large amount of Al and Cr ions, may be derived from deep seated sources.

I have also examined many tholeiitic and related basaltic and andesitic rocks of southwest Japan which contain no ultrabasic inclusion. Careful observation of these rocks has revealed that they also contain some amount of mafic xenocrystic minerals which were probably derived from ultrabasic rocks. For example, tholeiitic basaltic rocks from Shodoshima contains xenocrystic augite with spongy texture (YAMAGUCHI unpublished data). The Ôtozan Flow, composed

of basaltic and andesitic rocks also contains such abnormal crystals (YAMAGUCHI, 1958). The basalt collected from Kiuragi, Saga Prefecture contains zoned olivine with clear core, surrounded by bowlingite rim, and again of clear olivine developed around bowlingite. The olivine in this core may be regarded as xenocryst. Similar examples associating with ultrabasic inclusions have already been described in the previous section of this paper. Decomposition of clinopyroxene in nodules by the heat effect of magma may be expressed as follows.

Aluminian diopsidic augite (Table 7, No. 1)

$$Ca_{0.7}Na_{0.1}Mg_{0.8}Fe_{0.2}Al_{0.2}(Si_{1.8}Al_{0.2})O_6 = \underset{\text{Olivine}}{\begin{matrix}Mg_{0.8}Si_{0.4}O_{1.6}\\Fe_{0.2}Si_{0.1}O_{0.4}\end{matrix}} + \underset{\text{plagioclse}}{\begin{matrix}Na_{0.1}Al_{0.1}Si_{0.3}O_{0.8}\\Ca_{0.1}Al_{0.2}(Si_{0.1}Al_{0.1})O_{0.8}\end{matrix}} + \underset{\text{wollastonite}}{|Ca_{0.6}Si_{0.6}O_{1.8}|} + \underset{\text{silica}}{|(SiO_2)_{0.3}|} \quad \ldots(1)$$

$$Ca_{0.7}Na_{0.1}Mg_{0.8}Fe_{0.2}Al_{0.2}(Si_{1.8}Al_{0.2})O_6 + (SiO_2)_{0.2} = \underset{\text{augite}}{\begin{matrix}Mg_{0.8}Si_{0.8}O_{2.4}\\Fe_{0.2}Si_{0.2}O_{0.6}\\Ca_{0.6}Si_{0.6}O_{1.8}\end{matrix}} + \underset{\text{plagioclase}}{\begin{matrix}Na_{0.1}Al_{0.1}Si_{0.3}O_{0.8}\\Ca_{0.1}Al_{0.2}(Si_{0.1}Al_{0.1})O_{0.8}\end{matrix}} \quad \ldots\ldots\ldots\ldots\ldots(2)$$

in other word

Aluminian diopsidic augite $\longrightarrow$ olivine + plagioclase + silica + wollastonite molecule

Aluminian diopsidic augite + Silica $\longrightarrow$ augite + plagioclase

In silica undersaturated rocks, augite would be decomposed to aggregate of olivine and plagioclase (Fig. 8), releasing silica and wollastonite molecules. In silica saturated rocks, aluminian augite may react as to form augite and plagioclase. Such reactions may be controlled by the initial condition of the magma and eventually affect the course of crystallization of basalt magma.

It is an interesting fact that various kinds of volcanic rocks often enclose various kinds of holocrystalline nodules, of which the minerals and chemical compositions are similar to those of host volcanic rocks. The inclusions of what are called "cognate" are found in many other places as recorded in literature. Thus rhyolite often contains a siliceous inclusion, the hornblende andesite often contains a hornblende plagioclase inclusion (YAMAGUCHI unpublished data), the basaltic rocks often contain peridotitic and gabbroic inclusions (this paper, ROSS and others 1954, and many others). These kinds of evidence mean the closer genetical relationship of the inclusions to their host rock which is in many cases responsible for the interaction relation.

I have noted that the rock types of ultrabasic inclusions are variable from place to place and in different host rocks. Thus, limburgitic rocks abundantly contain dunite inclusions, the picritic basalt contains websterite inclusions, the olivine-basalt of Dôgo is characterized by the abundant olivine gabbro inclusions, and the olivine basalt of Karatsu contains abundantly various kinds of ultrabasic rocks. Many ultrabasic intrusive rocks are often layered, being composed of monomineralic rocks such as dunite, pyroxenite and other related rocks from a

layer to another. Such a layered structure is also expected at depth as indicated by the presence of strongly deformed ultrabasic inclusion of various rock types cmoposed largely of monomineralic rocks, and of layered peridotitic rocks. Probably, metamorphic differentiation played an important role in their formation.

The evidence seems to indicate that at least some basaltic and limburgitic rocks have come from different sources probably of different depth of the mantle, if the inclusions are really the products at these depth. The crystal-chemical characters of minerals in the inclusions would also support this explanation.

Conclusion

Many kinds of ultrabasic rocks enclosed in basaltic and limburgitic rocks dealt with in this paper are evidently fragments of consolidated rocks probably derived from different levels of layered ultrabasic rocks formed under stressed condition in the mantle.

The inclusions are often disintegrated and their constituent minerals are dispersed throughout the magma. Some of the minerals which are no longer stable in the magma tend to make structural adjustment to the physical condition which has been imposed on the magma and which differs from the condition under which the inclusions in question originated. Again, the predominant rock types of various inclusions in a given host rock often present a certain similarity in mineralogy to their host rock. This indicates that there is a possibility of their close petrogenic relationships involving chemical adjustment of the constituent minerals of the inclusion to the chemical composition of the magma.

Many of the peridotitic intrusive rocks which are met with in the accessible part of the crust have often been considered as the representatives of the earth's peridotite mantle. However, the packing index of clinopyroxenes and other physical-chemical featurs of the inclusions indicate that most peridotitic intrusive rocks should be distinguished from the ultrabasic inclusions in question. In other words, the ultrabasic rocks included in basaltic rocks seem to have been derived from greater depths, comparatively deeper than the source of peridotitic intrusive rocks.

Locality Guide

	East Long.	North Lat.
Hinodematsu (日の出松)	128°54′	33°28′
Ariura-mura, Higashi-matsu-ura-gun, Saga Prefecture (佐賀県東松浦郡有浦村)		
Kajikoyama (加治子山)	133°50′	35°03′
Ôi-nishi-mura, Kume-gun, Okayama Prefecture (岡山県久米郡大井西村)		
Kurose (黒瀬)	130°10′	33°10′
Rock at the mouth of Hakata Bay, Fukuoka City (福岡市博多湾内岩礁)		
Kyonomatsu (京の松)	129°53′	33°28′

Ariura-mura, Higashi-matsu-ura-gun, Saga Prefecture (佐賀県東松浦郡有浦村)

Meyama (女山) ..... 133°56′ 35°06′
Ariura-mura, Higashi-matsu-ura-gun, Saga Prefecture (岡山県久米郡大野村土居)

Nochi (野馳) ..... 133°19′ 34°55′
Nochi-mura, Atetsu-gun, Okayama Prefecture (岡山県阿哲郡野馳村)

Ôguso-yama (大糞山) ..... 132°01′ 34°48′
Shimo-ima-myo, Ino-mura, Naka-gun, Shimane Prefecture (島根県那賀郡井野村下今明)

Ôga (相賀) ..... 129°57′ 33°30′
Karatsu City, Saga Prefecture (佐賀県唐津市)

Oyama (男山) ..... 133°56′ 35°06′
Doi, Ôno-mura, Kume-gun, Okayama Prefecture (岡山県久米郡大野村土居)

Shimo-ganya (下元屋) ..... 133°17′ 36°18′
Nakamura, Dôgo, Oki Islands, Suki-gun, Shimane Prefecture (島根県周吉郡隠岐島後中村)

Sukumozuka (稼塚) ..... 133°55′ 35°03′
Shitori-higashi-mura, Kume-gun, Okayama Prefecture (岡山県久米郡倭文東村)

Takashima (高島) ..... 129°59′ 33°28′
Islet in the Karatsu Bay, Karatsu City, Saga Prefecture (佐賀県唐津市唐津湾内)

References Cited

AOKI, Ken-ichiro (1959): Petrology of alkali rocks of the Iki Islands and Higashi-matsuura district, Japan. *Sci. Rep. Tohoku Univ.* Ser. III, **6**, (2), 261–310.

AOYAMA, Nobuo (1942): Large crystals of clino-pyroxene in the basalt from Takashima, (Abstract in Japanese). *Jour. Geol. Soc. Japan*, **49**, (585), 206–207.

BOWEN, N. L. (1928): *The Evolution of the Igneous Rocks*. Princeton University Press, 332 pp.

———, and TUTTLE, O. F. (1949): The system MgO–SiO_2–H_2O. *Bull. Geol. Soc. Am.*, **60**, 439–460.

BROWN, G. M. (1957): Pyroxenes from the early and middle stage of fractionation of the Skaergaard intrusion, East Greenland. *Min. Mag.*, **31**, 511–543.

———, (1960): The effect of ion substitution on the unit cell dimensions of the common clinopyroxenes. *Am. Mineral.*, **45**, 15–38.

BUDDINGTON, A. F. (1943): Some petrological concepts and the interior of the earth. *Am. Mineral.*, **28**, 119–140.

ESKOLA, P. (1933): On the differential anatexis of rocks. *Compt. Rend. Soc. Géol. Finlande*, No. 7, 12–25.

FAIRBAIRN, H. W. (1943): Packing in ionic minerals. *Bull. Geol. Soc. Amer.*, **54**, 1305–1374.

FERMOR, L. L. (1914): The relationship of isostasy, earthquake, and volcanicity to the earth infra-plutonic shell. *Geol. Mag.* Decade VI, **1**, 65–67.

HARADA, Zyumpei (1943): On the chrome minerals of Japan (II) (in Japanese). *Jour. Jap. Assc. Mineral. Petrol. Econ. Geol.*, **29**, (1), 12–23.

HARUMOTO, Atsuo (1951): Limburgite from Sukumozuka in the vicinity of Tsuyama, Okayama Prefecture (Abstract in Japanese). *Jour. Geol. Soc. Japan*, **57**, 318.

———, (1952): Melilite-nepheline basalt, its olivine nodules, and other inclusions from Nagahama, Japan. *Mem. Coll. Sci. Kyoto Univ.* [B], **20**, (2), 69–88.

HESS, H. H. (1949): Chemical composition and optical properties of common clinopyroxenes. *Am. Mineral.* **34**, 621-666.

——— (1960): Stillwater igneous complex, Montana. *Geol. Soc. America Memoir*, 80, 230pp.

——— and HENDERSON, E. P. (1949): The Moore County meteorite: A further study with comment on its primordial environment. *Am. Mineral.*, **34**, 494-507.

——— and PHILLIPS, A. H. (1938): Orthopyroxenes of the Bushveld Type. *Am. Mineral.*, **23**, 450-456.

HOLMES, A. (1932): The origin of igneous rocks. *Geol. Mag.*, **69**, 543-558.

JOLY, J. (1925): *Surface History of the Earth*, Oxford: The Clarendon Press, 192 pp.

KUNO, Hisashi and NAGASHIMA, Kozo (1952): Chemical composition of hypersthene and pigeonite in equilibrium in magma. *Am. Mineral.* **37**, 1000-1006.

——— and HESS, H. H. (1953): Unit cell dimensions of clinoenstatite in relation to other common clinopyroxenes, *Am. J. Sci.*, **251**, 741-752.

——— (1953): Recent trends of igneous petrogenesis (in Japanese). *Kagaku*, **23**, (2), 66-71.

——— (1955): Ion substitution in the diopside-ferropigeonite series of clinopyroxenes. *Am. Mineral.*, **40**, 70-93.

——— (1957): Chromian diopside from Sano, Yamanashi Prefecture. *Jour. Geol. Soc. Japan*, **63**, (744), 523-526.

——— (1959a): Origin of Cenozoic petrographic provinces of Japan and surrounding areas. *Bull. Volcanologie*, Ser. II, **20**, 37-76.

——— (1959b): Discussion of paper by J. F. LOVERING, 'The nature of the Mohorovičič Discontinuity'. *Jour. Geoph. Research*, **64**, (8), 1071-1072.

——— (1960): High-alumina basalt. *Jour. Petrology*, **1**, (2), 121-145.

KOBAYASHI, Isamu, IMAI, Isao and MATSUI, Kazunori (1955): *1:50,000 geological sheet map and explanatory text of the Yobuko* (in Japanese with English abstract). Geol. Surv. of Japan, 28 pp.

———, ———, ——— (1956): *1:50,000 geological sheet map and explanatory text of the Karatsu* (in Japanese with English abstract). Geol. Surv. of Japan, 60 pp.

KOZU, Syukusuke (1913): Petrological notes on the igneous rocks of the Oki Island. *Sci. Rep. Tohoku Imp. Univ.*, Second Ser., **1**, p. 51.

LOVERING, J. F. (1958): The nature of the Mohorovičič discontinuity. *Trans. Am. Geophys. Union*, **39**, 947-955.

——— (1959): Author's reply to preceding discussion (Letter to the editor, Discussion of paper "The nature of the Mohorovicic discontinuity"). *Jour. Geoph. Research*, **64**, (8), 1073.

MACDONALD, G. A. (1941): Progressive metasomatism of serpentine in the Sierra Nevada of California. *Am. Mineral.*, **26**, 276-287.

——— (1942): Geology of the western Sierra Nevada between the Kings and San Joaquin rivers, California. *Bull. Dept. Geol. Univ. Califlornia*, **26**, 244.

——— (1961): Volcanology. *Science*, **133**, (3454), 673-679.

MASON, B. H. (1952): *Principles of Geochemistry*. John Wiley & Sons, New York, 276 pp.

MORIMOTO, Nobuo and ITO, Teiichi (1958): Pseudo-twin of augite and pigeonite (Abstract of paper submitted for the meeting in St. Louis, Missouri). *Bull. Geol. Soc. Am.*, **69**, (12-2), 1616.

MIYAKE, Terumi (1948): Reexamination of clinopyroxenes from Nishigatake (in Japanese). *Mineralogy and Geology*, **2**, (Series 8), 77-80.

NORTON, D. A., and CLAVAN, W. S. (1959): The optical mineralogy, chemistry and X-ray crystallography of ten clinopyroxenes from the Pennsylvania and Delaware Piedmont Province. *Am. Mineral.*, **44**, 844-874.

O'HARA, J. M. and MERCY, L. P. (1963): Petrology and petrogenesis of some garnetiferous peridotites. *Trans. Royal Soc. Edinburgh*, LXV, (12), 251-314.

ÔJI, Yoshio (1961a): On the augite phenocryst in alkali basalts from the Abu district (in Japanese with English abstract). *Jour. Japanese Assoc. Mineral. Petrol. Econ. Geolo-*

gists, **45**, (2), 66–70.

——— (1961b): Olivines in the alkali-basalts of western San-in and northern Kyushu (in Japanese with English abstract). *Jour. Japanese Assoc. Mineral. Petrol. Econ. Geologists*, **45**, (4), 133–136.

POLDERVAART, A. (1947): The relationship of orthopyroxene to pigeonite. *Min. Mag.*, **28**, 164–172.

——— and HESS, H. H. (1951): Pyroxenes in the crystallization of basaltic magma. *Jour. Geol.*, **59**, 472–489.

PAULING, L. (1960): *Nature of the Chemical Bond.* Cornell Univ. Press, 2nd edition, 644pp.

POWERS, H. A. (1955): Composition and origin of basaltic magma of the Hawaiian Islands. *Geochim. et Cosmochim. Acta*, **7**, 77–107.

REED, H. H. (1934): On zoned associations of antigorite, talc, actinolite, chlorite, and biotite in Unst, Shetland Islands. *Min. Mag.*, **23**, (145), 519–540.

ROSS, C. S., FOSTER, M. D., and MYERS, A. T. (1954): Origin of dunites and of olivine-rich inclusions in basaltic rocks. *Am. Mineral.*, **39**, 693–737.

SEKI, Yotaro (1951): Metamorphism of ultrabasic rocks caused by intrusion of granodiorite in Miyamori district, Iwate Prefecture—Metamorphism of serpentine rock (in Japanese with English abstract). *Jour. Geol. Soc. Japan*, **57**, (2), 35–43.

SMYTHE, J. A. (1914): On some inclusions in the great Whin Sill of Northumberland. *Geol. Mag.* Decade VI, **1**, 244–254.

SUGI, Ken-ichi (1940): On the nature of some plagioclase with apparently small optical angle, with special reference to the plagioclase in olivine dolerite from Fu-Shun, Manchuria. *Mem. Fac. Sci., Kyushu Imp. Univ.* [D], **1**, (1), 1–22.

——— (1942): Petrological studies on the basaltic rocks from San-in and Northern Kyūshū, Southwestern Japan, Part I. *Mem. Fac. Sci. Kyūshū Imp. Univ.* [D], **1**, (3), 69–90.

——— (1951a): Diallage and its inclusions in gabbro from Ayabe, Tamba Province, Japan (in Japanese). *Sci. Rep. Fac. Sci. Kyushu Univ. Geol.*, **3**, (2), 1–5.

——— (1951b): Contamination origin of the tholeiites associated with the olivine basalt in the San-in and North Kyushu regions, Southwest Japan (in Japanese). *Sci. Rep. Fac. Sci. Kyushu Univ. Geol.*, **3**, (2), 7–12.

TILTON, G. R., WETHERILL, G. W., ALDRICH, L. T., DAVIS, G. L. and JEFFERY, P. M. (1956): Age of ancient minerals. *Carnegie Inst., Washington 1955–1956 Year Book*, no. 55, 87–100.

TOMITA, Toru (1927–1932): Geological and petrological study of Dôgo, Oki (in Japanese). *Jour. Geol. Soc. Tokyo*, **34** (1927), 321–338 (Part 1), 423–460 (Part 2); **35** (1928), 463–491 (Part 3), 519–537 (Part 4), 571–600 (Part 5); **36** (1929), 189–205 (Part 6), 303–337 (Part 7); **37** (1930), 131–156 (Part 8), 521–546 (Part 9); **38** (1931), 155–174 (Part 10), 203–222 (Part 11), 413–431 (Part 12), 461–475 (Part 13), 545–564 (Part 14), 609–628 (Part 15); **39** (1932), 149–178 (Part 16), 197–219 (Part 17), 501–523 (Part 18), 609–640 (Part 19), 675–691 (Part 20).

——— (1935): On the chemical compositions of Cenozoic alkaline suite of the Circum Japan Sea region. *Jour. Shanghai Sci. Institute*, Sec. II, **1**, 227–306.

——— (1936): Geology of Dôgo, Oki Islands, in the Japan Sea. *Jour. Shanghai Sci. Inst.*, Sec. II, **2**, 37–146.

——— (1951): Peneplain of Higashi-Matsuura district and its geological significance (abstract in Japanese). *Rep. West Japan Branch Geol. Soc. Japan*, No. 8, 4.

——— (1954): Geologic significance of the colour of granite zircon, and the discovery of Pre-Cambrian in Japan. *Mem. Fac. Sci. Kyushu Univ.*, [D], **4**, 135–161.

——— (1956): Radioeffect in zircon (in Japanese with English abstract). *Chikyu Kagaku* (*Earth Science*), No. 26–27, 36–51.

——— (1958): Chemical distinctions between the three principal series of basaltic rocks (in Japanese with English abstract). *Jubilee Publication in Commemoration Professor Jun SUZUKI, M. J. A. Sixtieth Brithday* (1956), 193–211; translated into English by Reiko FUSEJIMA, *International Geol. Review*, **2**, (11), 967–982.

TURNER, F. J. (1942): Preferred orientation of olivine crystals in peridotite, with special reference to New Zealand examples. *Roy. Soc. New Zealand, Transactions*, **72**, Part 3, 280–300.

——— and VERHOOGEN, J. (1951): *Igneous and Metamorphic Petrology*. Mc. Graw-Hill Book Co., New York, 602 pp.

WAGER, L. R. (1958): Beneath the earth's crust. *Advance of Sci.*, **15**, 31–45.

WALKER, F., and POLDERVAART, A. (1949): Karro dolerites of the Union of South Africa. *Bull. Geol. Soc. Amer.*, **60**, 591–706.

WASHINGTON, H. S. (1917): Chemical Analysis of Igneous Rocks. *U.S. Geol. Survey Prof. Paper*, No. 99, 625.

WILSHIRE, H. G. and BINNS, R. A. (1960): Basic and ultrabasic xenoliths from volcanic rocks of New South Wales. *Jour. Petr.*, **2**, 185–208.

YAMAGUCHI, Masaru (1958): Petrography of the Otozan Flow on Shodo-shima Island, Setouchi Inland Sea, Japan. *Mem. Fac. Sci. Kyushu Univ.* [D], Geol., **6**, (3), 217–238.

——— (1961a): Chrome-diopsides in the Horoman and Higashi-Akaishi peridotites, Japan. *Mem. Fac. Sci. Kyushu Univ.* [D], Geol., **10**, (2), 233–245.

——— (1961b): Nodules in andesite from Matsubara, south of Hita City, Ôita Prefecture, Japan (in Japanese with English abstract). *Sci. Rep. Fac. Sci. Kyushu Univ.*, Geol. Ser., **5**, (3), 149–164.

YODER, H. S., and TILLEY, C. E. (1962): Origin of basalt magma: An experimental study of natural and synthetic rock systems. *Jour. Petr.* **3**, 342–532.

Masaru YAMAGUCHI

Petrogenic Significance of Ultrabasic Inclusion

Plates 22–26

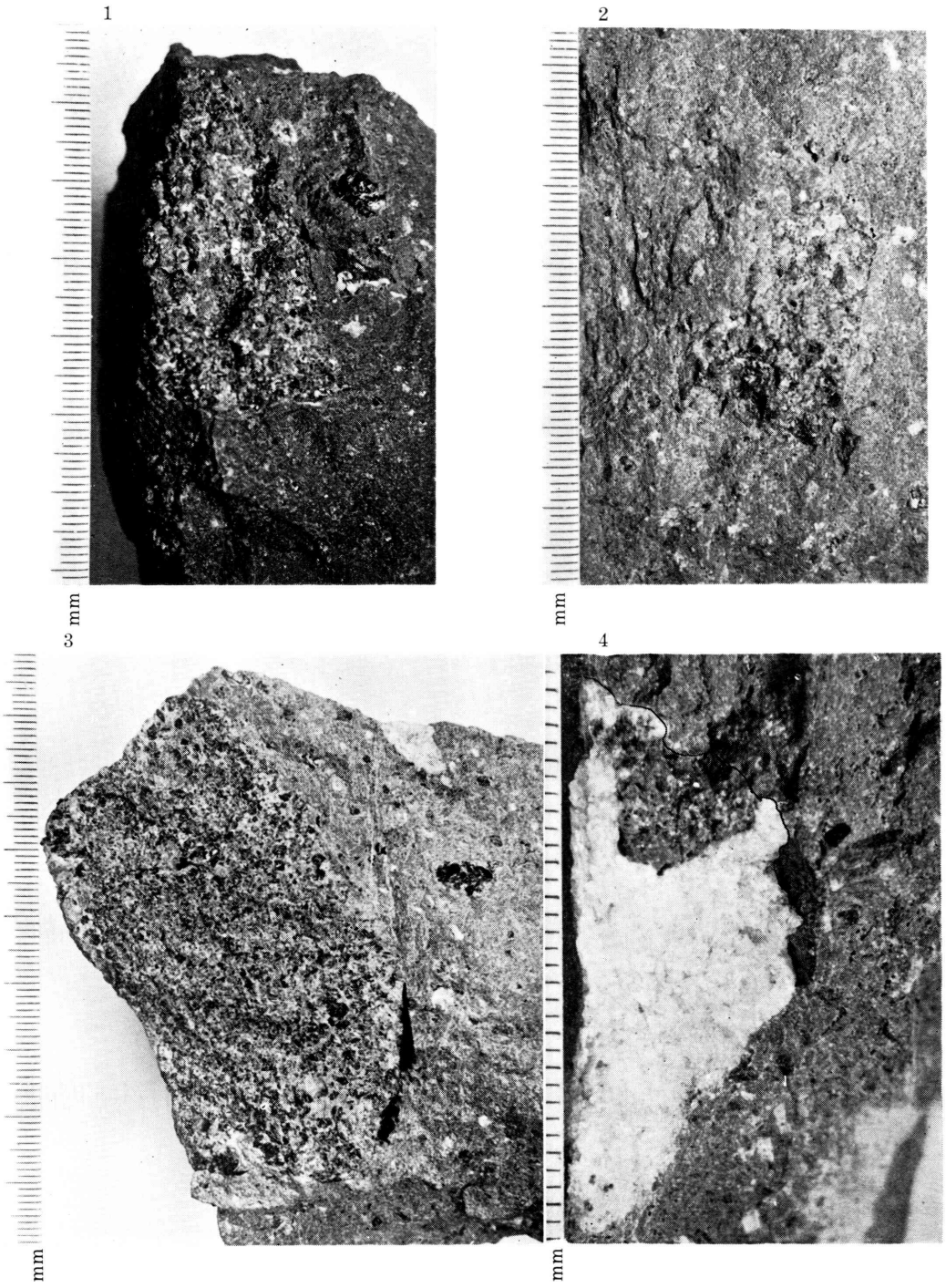

Photomacrographs of handspecimens of ultrabasic inclusions in olivine basalt from Shimoganya, Dôgo, Oki Islands

1. Wehrlite inclusion 2. Harzburgite inclusion 3. Websterite inclusion
4. Wehrlite inclusion surrounded by anorthosite (white area)

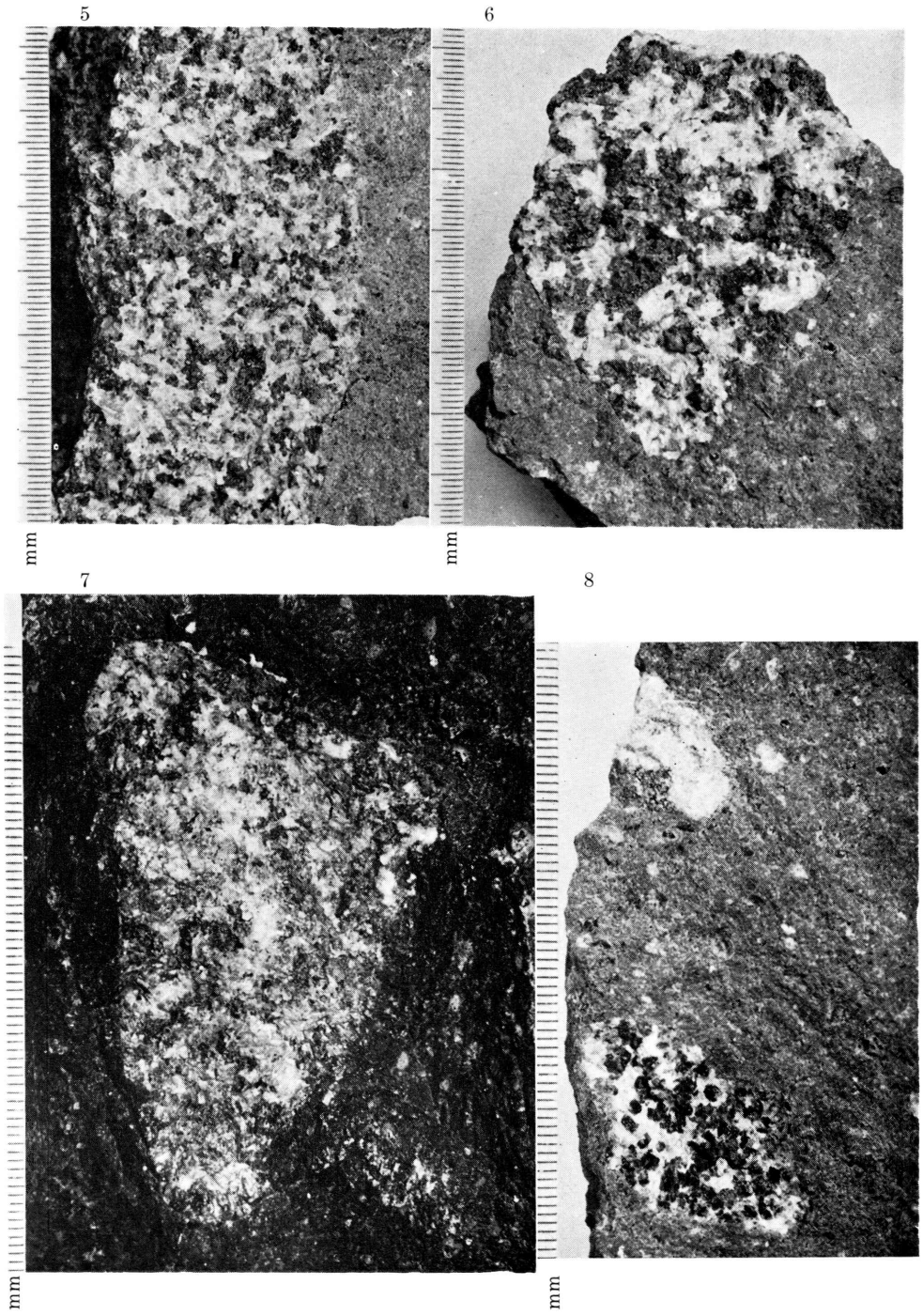

Photomacrographs of handspecimens of ultrabasic inclusions in olivine basalt from Shimoganya, Dôgo, Oki Islands

5. Olivine gabbro inclusion 6. Augite olivine gabbro inclusion 7. Augite olivine gabbro inclusion. 8. Augite olivine gabbro inclusion (lower) and quartzite inclusion (upper)

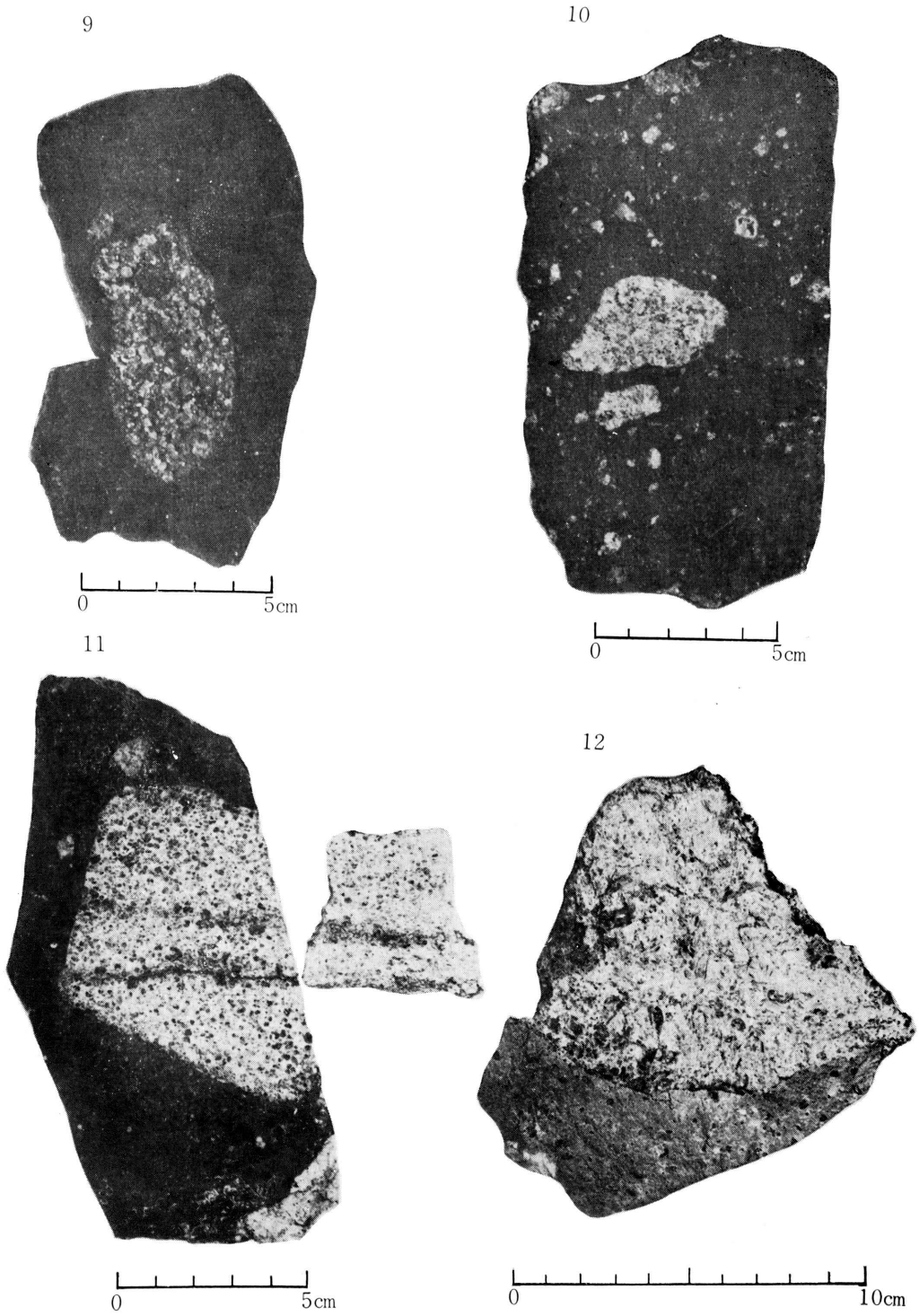

Photomacrographs of handspecimens of ultrabasic inclusion

9. Dunite inclusion in olivine basalt from Takashima Islet, Saga Prefecture. 10. Peridotite inclusion in limburgite from Ôguso-yama, Shimane Prefecture. 11. Peridotite inclusion in olivine basalt from Hinodematsu, west of Karatsu City showing layering of minerals. Darker layer contains larger amount of green diopside (polished surface). 12. Diallagite inclusion in olivine basalt from Hinodematsu.

13

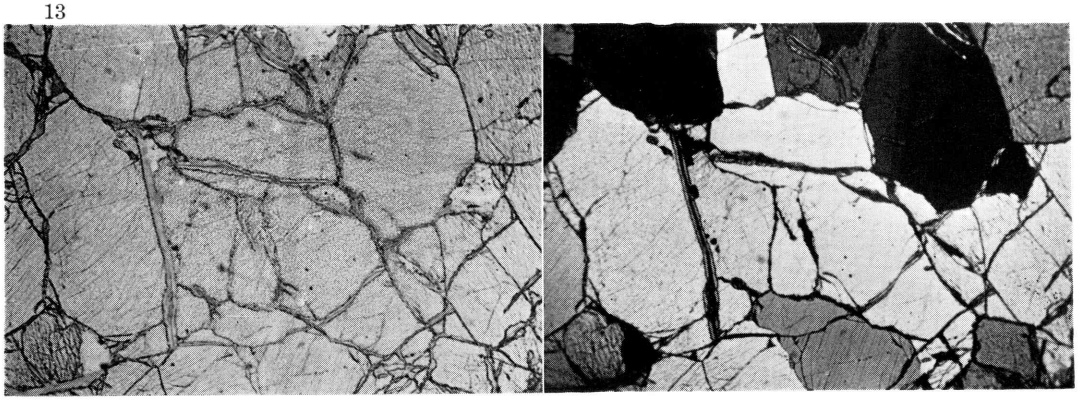

14 0 0.5mm

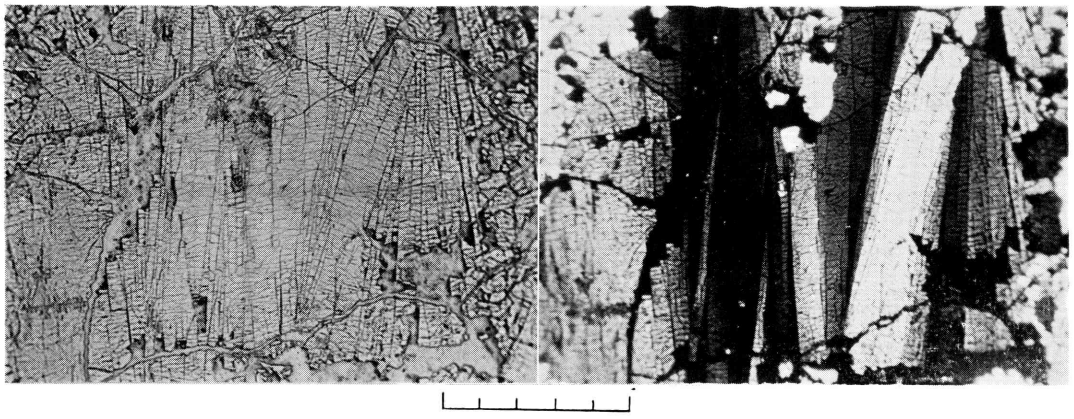

15 0 0.5mm

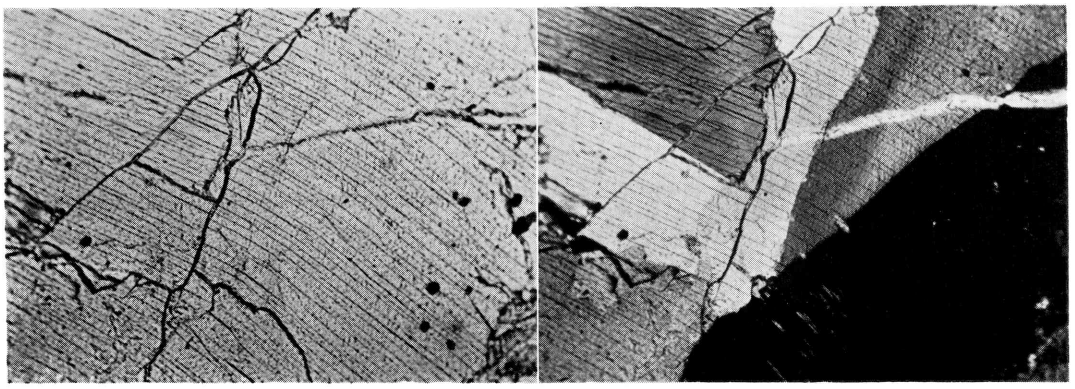

0 0.5mm

Photomicrographs of ultrabasic inclusion (left; open, right; crossed Nicols)

13. Dunite inclusion in olivine basalt from Takashima Islet showing translation lamellae of olivine 14. Strongly strained olivine crystal of peridotite inclusion in limburgite from Ôgusoyama, showing fine translation lamellae 15. Aluminian diopsidic augite of diallagite inclusion in oilivne basalt from Hinodematsu. Note the bending of cleavage plane, undulose extinction and the exsolution lamellae (in the lower part) of bronzite.

16A

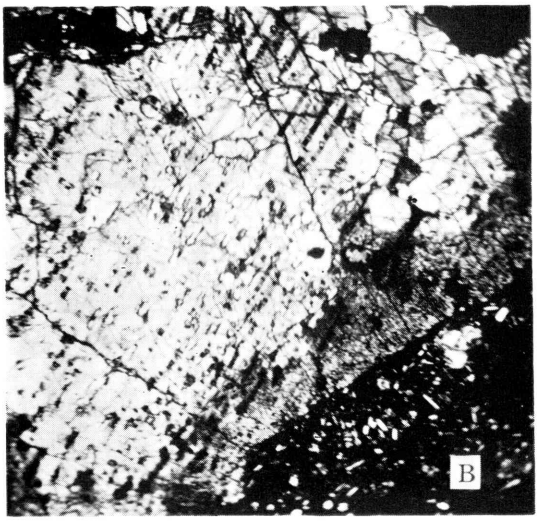

1 mm

16B

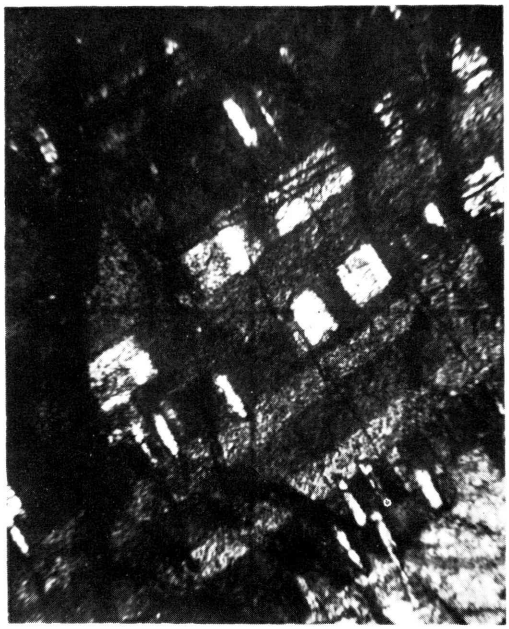

0.1mm

16C

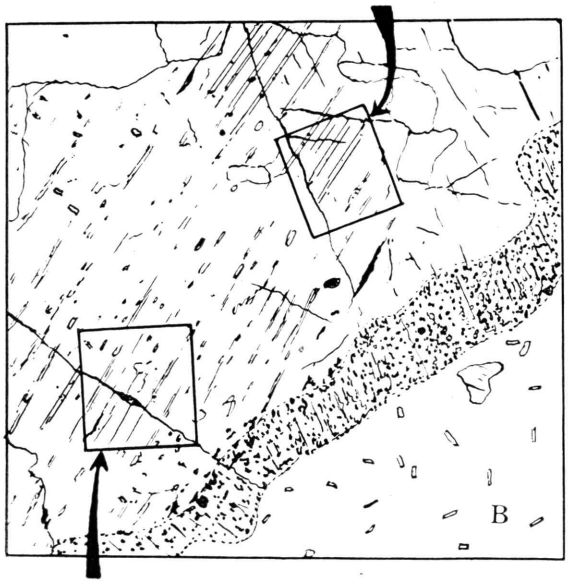

0.2mm

Photomicrographs showing the exsolution pattern of aluminian diopsidic augite from websterite inclusion in picrite-basalt from Nochi, Okayama Prefecture (crossed Nicols). Note the spongy rim of the augite along the contact of host basalt (B).